THE STUDY OF SONIC HEDGEHOG SIGNALING PATHWAY IN THE DEVELOPMENT OF LYSOSOMAL ACID PHOSPHATASE (ACP2) MUTANT MICE CEREBELLAR GRANULE CELLS

BY

XIAODAN JIAO

A Thesis Submitted to the Faculty of Graduate Studies of
The University of Manitoba
in Partial Fulfillment of the Requirements for the Degree of

MASTER OF SCIENCE

Department of Human Anatomy and Cell Science
University of Manitoba
Winnipeg, Manitoba

ABSTRACT

A lysosomal acid phosphatase 2 (Acp2) mutant mouse (naked-ataxia, *nax*) shows severe cerebellar cortex defect with a significant reduction in granule cells in the cerebellum. The sonic hedgehog (SHH) and N-Myc pathways are important for granule cell precursor proliferation and differentiation. The project tests the hypothesis that the proliferation defect of granule cells is associated with SHH - N-Myc pathway impairment in the *nax* mutant cerebellum. To investigate morphological changes in the *nax* cerebellum and alteration in the SHH - N-Myc pathway, *in vivo* and *in vitro* immunohistochemistry and Western blotting were used. My data showed a strikingly reduced N-Myc expression in the *nax* cerebellum, which was accompanied by an increase in proteasome activity, suggesting that the significant reduction of granule cells in *nax* cerebellum is potentially due to the dysregulation of N-Myc via the abnormal ubiquitin-proteasome system activity.

ACKNOWLEDGEMENTS

To my supervisor, Dr. Hassan Marzban, thank you for your accepting me into your laboratory and the kindest support to assist me to finish this research. Dr. Marzban was always patient, understanding and encouraged me to continue my education. Not only on the scientific research, Dr. Marzban also provided the opportunity to work as a teaching assistant to improve my work experience.

To my committee member, Dr. Efterhar Efterharpour, thank you for your kindest advice regarding my study and my life. Your suggestion on how to balance the work and life helped me builds the foundation for my three-year research in Canada. Dr. Jiming kong who regards me as his family kindly supported my study and life during these three years. I would like to give a special thanks to you for your recommendation to pursue my dream in Canada at the very first beginning. Dr. Maria Vrontakis, thank you for your persistent encouragement and compliment which gave me the confidence to continue my research.

To Dr. Saeid Ghavami thank you for your generous guidance on the cell culture experiment.

And I would like to thank Dr. Sanjiv Dhingra and Ejlal Abuelrub from St. Boniface Hospital research center who helped me to fulfill the proteasome activity experiment in this research project.

To my lab members Maryam Rahimi Balaei and Niloufar Ashtari, who are definitely

my good friends, thank you for helping and supporting me in the learning and accomplishing the experiments in our warm laboratory. Hope to continue work with you and wish you success in your future.

I would like to thank my friends who provided enriched cultural and recreational activities besides my study and encouraged me to achieve this research.

And my dearest family, many thanks to you for your endless love, understanding and support. I am so sorry that I am far away from you and not able to being with you when you need me. And my lovely dog Sibao, thank you for joining my family, bringing the joyousness and accompanying with my parents instead of me.

This Master research would not have been achieved without all your support and I am really appreciated what you have done for me.

TABLE OF CONTENTS

LIST OF TABLES

LIST OF FIGURES

ABBREVIATIONS

ACC: Animal Care Committee

Acp2: Lysosomal acid phosphatase 2

BDNF: brain-derived neurotrophic factor

BMPs: Bone morphogenetic protein

CaBP: Calcium-binding protein

CCAC: Canadian Council for Animal Care

CNS: central nervous system

CSF: cerebrospinal fluid

DAB: Diaminobenzidine

DHH: Desert hedgehog

E: embryonic day

E1: ubiquitin-activating enzyme

E2: ubiquitin-conjugating enzyme

E3: ubiquitin ligase

ECL: electrochemiluminescence

EGZ: external germinal zone

FGF: Fibroblast growth factor

GABA: gamma-Aminobutyric acid (γ-Aminobutyric acid)

gcl: granule cell layer

GFAP: Glial fibrillary acidic protein

GLHS: Gomez Lopez Hernandez syndrome

Gli: glioma-associated oncogene homolog

h: hemisphere

hh: hedgehog gene

IHH: Indian hedgehog

IPI-926: saridegib

LAP: Lysosomal acid phosphatase 2

ME: mercaptoethanol

MEFs: Mouse Embryonic Fibroblasts

ml: molecular layer

nax: naked-ataxia

N-Myc: N-Myc proto-oncogene protein

NTZ: nuclei transitory zone

P: postnatal

Pax-6: Paired box protein 6

PBS: phosphate buffer saline

pcl: Purkinje cell layer

PCR: Polymerase Chain reaction

PFA: paraformaldehyde

PTCH1: Protein patched homolog 1

r1: rhombomere 1

RL: rhombic lip

SHH: Sonic Hedgehog

SHH-N: N-terminal signaling domain of Sonic hedgehog

SHH-C: C-terminal signaling domain of Sonic hedgehog

SMO: Smoothened

SSD: sterol sensing domain

SUFU: Suppressor of fused homolog

UBCs: Unipolar Brush cells

v: vermis

VZ: ventricular zone

wt: wild-type

CHAPTER 1: INTRODUCTION

1.1 Cerebellum

The cerebellum is a brain region with very important roles in motor control and cognition (Steinlin; Thach; Wolf, Rapoport and Schweizer). The cerebellum motor function includes equilibrium, posture, coordination, fine movement and motor learning (Fine, Ionita and Lohr). There are increasing findings and evidence proving that cerebellum is not purely motor-related; it is also involved in cognitive functions including language, attention, and mental imagery (Fine, Ionita and Lohr; Doya).

The human cerebellum attaches posteriorly to the brain stem and is located underneath the cerebral hemispheres. Like the cerebrum, the cerebellum has two lateral hemispheres. It also has a vermis which is located at the midline. The cerebellum can be divided into 3 lobes (anterior lobe, posterior lobe and flocculonodular lobe) according to the external feature and further subdivided into 10 lobules (Llinas and Negrello).

The cerebellum consists of an assembled three-layered cortex including molecular layer (ml), Purkinje cell layer (Pcl), and granule cell layer (gcl) and the cerebellar nuclei that are embedded in white matter (Marzban et al.; Llinas and Negrello). The granule cell layer is packed with numerous granule cells which comprise approximately 80% of the central nervous system neurons. The granule cell layer also comprises Golgi cells and Unipolar Brush cells (UBCs) (Azevedo et al.). The second layer is Purkinje cell layer that mainly consists of a single layer of Purkinje cell somas accompanied by the Bergmann glial cell bodies (Llinas and Negrello). The molecular layer is the most superficial layer

contains dendritic trees of Purkinje cells, parallel fibers of granule cells axon, stellate cells, basket cells, and Bergmann glial fibers (Llinas and Negrello; Marzban et al.; Azevedo et al.). The three pairs of cerebellar nuclei (dentate, interposed (globose, emboliform), and fastigial) lie in the white matter which are the sole output of the cerebellum accompanied by lateral vestibular nucleus (Llinas and Negrello; Marzban et al.). The mossy fibers afferent synapse with granule cells dendrites. The axons of the granule cells project toward the molecular layer and form parallel fibers which exert the excitatory effect on the Purkinje cell dendrites. The Purkinje cells axons, sole output of the cerebellar cortex, project to the cerebellar nuclei. Another set of afferent fibers to the cerebellum is called climbing fibers and responsible for carrying the input from the inferior olivary nuclei to the Purkinje cells (Llinas and Negrello).

1.2 Development of central nervous system (CNS)

The majority of neurons and glial cells of central nervous system originate from the neural plate which is formed by the epiblast of the embryo during early development (Smith and Schoenwolf; Gray and Ross). At the fourth week of the development in human and around E7-7.5 in mouse, the neural plate folds to generate the neural tube which is later filled with cerebrospinal fluid (CSF) (Gray and Ross; Smith and Schoenwolf). The anterior (rostral) neural tube forms vesicles which generates the different brain regions: the forebrain (prosencephalon) which is then divided into telencephalon and diencephalon, the midbrain (mesencephalon) and the hindbrain

(rhombencephalon) which are further subdivided into the metencephalon (future pons and cerebellum) and myelencephalon, from which the medulla oblongata develops. The posterior (caudal) part of the neural tube forms the spinal cord (Wurst and Bally-Cuif; Teng et al.). During embryonic development, some of the neural stem cells which are located in the wall of neural tube switch from proliferative phase into differentiation to form the neurons and glial cells. These neurons and glial cells migrate to their destination and communicate with other neurons via their dendrites or axons (Rakic). Many different signaling molecules are involved in the patterning of the nervous system. Sonic Hedgehog (SHH) is responsible for ventralization (the formation of ventral neural tube), and induces neurons to differentiate into motor neurons and ventral interneurons. The dorsal neural tube (alar plate) is regulated by Bone morphogenetic protein (BMPs) and gives rise to the sensory interneurons. The rostrocaudal neural tube patterning is regulated by Fibroblast growth factor (FGF) and retinoic acid (Duester; Martinez-Ferre and Martinez; Lee and Jessell; Echelard et al.).

1.3 Development of the cerebellum and neurogenesis

Both in humans and lower mammals, the development of the cerebellum starts from the embryonic period and extends well into the early postnatal life. During the neural tube closure, the anlage of the cerebellum (cerebellar primordium) is developed from rhombomere 1 (r1), a region that all the cells of the cerebellum arisen from (Nakamura et

al.). Müller and O'Rahilly described the development of the cerebellum with detailed morphologic descriptions during embryonic stages (Eccles, Llinas and Sasaki; Muller and O'Rahilly "The Human Brain at Stage 16, Including the Initial Evagination of the Neurohypophysis"; Muller and O'Rahilly "The Human Brain at Stages 18-20, Including the Choroid Plexuses and the Amygdaloid and Septal Nuclei"; Muller and O'Rahilly "The Human Brain at Stages 21-23, with Particular Reference to the Cerebral Cortical Plate and to the Development of the Cerebellum"). In human, at Carnegie stage 14 (32 days) the cerebellar primordium forms but its two sides are not yet connected and there is a gap in between the two hemi cerebellar primordia (Bogaert and Belpaire). The rhombic lip, an important cerebellar germinal zone, is established at stage 16 (40 days) (Muller and O'Rahilly "The Human Brain at Stage 16, Including the Initial Evagination of the Neurohypophysis"). At stage 18-19 (44-48 days) neuroepithelial-derived neural progenitors start migrating from the ventricular zone (VZ) (Muller and O'Rahilly "The Human Brain at Stages 18-20, Including the Choroid Plexuses and the Amygdaloid and Septal Nuclei") to the core of the cerebellar primordium. The external germinal zone (EGZ) is formed at the dorsum of the cerebellum due to the migration of granule cell precursors from the rhombic lip at stage 23 (57 days) (Muller and O'Rahilly "The Human Brain at Stages 21-23, with Particular Reference to the Cerebral Cortical Plate and to the Development of the Cerebellum").

As mentioned above, the cerebellar primordium is formed from rhombomere 1 which is a region definitively characterized by lacking the expression of *Otx2* (rostral limit) and

Hoxa2 genes (caudal limit) (Butts, Green and Wingate). The isthmus, a narrowed area of the neural tube between mesencephalon and rhombencephalon, provides different important signaling molecules to regulate the development of cerebellar primordium such as OTX2, Wnt1, En1/2, and FGF8 (Wassarman et al.; Katahira et al.; Heikinheimo et al.).

1.4 Cerebellar germinal zones

Diverse types of the cerebellar neurons originate from different germinal zones: ventricular zone (VZ), rhombic lip (RL), and probably from a new germinal zone at the rostral end (mesencephalon). Ventricular zone and rhombic lip generate cerebellar glutamatergic and GABAergic neurons, respectively (Leto et al.).

1.4.1 Ventricular zone

The ventricular zone is the wall of the alar plate in the rostral end of the rhombencephalon or the neuroepithelium of the fourth ventricle. Purkinje cells, Golgi cells, and all interneurons that are considered cerebellar GABAergic neurons originate from the ventricular zone (Marzban et al.).

1.4.1.1 Purkinje cell

Purkinje cells are amongst the largest neurons in the human brain named after the Czech anatomist Jan Evangelista Purkyně who firstly described this cell (Llinas and Negrello). Purkinje cells are characterized by an elaborate dendritic arbor with a large

number of dendritic spines. The Purkinje cell somas are arranged in a monolayer (one cell thick) called Purkinje cell layer in the cerebellar cortex. The large dendritic tree synapses with the parallel fibers of granule cells in the molecular layer. Around 150,000 to 200,000 parallel fibers synapse with a single Purkinje cell dendrite (Tyrrell and Willshaw). Besides the parallel fibers, Purkinje cells also receive excitatory synapses from climbing fibers (Wadiche and Jahr). Because Purkinje cells serve as the sole output of cerebellar cortex with inhibitory projection to the cerebellar nuclei, they are considered to play a central role in the cerebellar cortex (Mishina et al.; Chaumont et al.).

In human, during the gestation weeks 12 to 16, Purkinje cells are small and disperse from cluster stage to form monolayer and their dendrites develop, while synapse with other neurons between 16 to 28 weeks (Zecevic and Rakic). The volume of Purkinje cells quickly increases in the first two years and reaches the adult size around 7 to 9 years old (Tsekhmistrenko). However, the Purkinje cells are generated at E10-E13 in mouse and then form the multilayer at E14-P1 which will eventually disperse to a monolayer around P4-P7 (Marzban et al.).

1.4.1.2 Golgi Cells

Golgi cells are the inhibitory interneurons located in the granule cell layer of the cerebellum (Eccles, Llinas and Sasaki). There are two different types of Golgi cells based on their size in cerebellar granular layer. The larger one is mainly located in the upper part of the granule cell layer and Golgi cell with smaller size is found in the lower part of

the granule cell layer (Llinas and Negrello). Their extensive dendritic processes pass through all three layers of the cerebellar cortex and synapse with granule cells parallel fibers which are excitatory input. In addition, Golgi cells synapse directly with mossy fibers and granule cell dendrites to form the cerebellar glomeruli which are excitatory input (Jakab and Hamori). Using GABA neurotransmitter, the Golgi cells can transport feed-forward and feed-back inhibition of granule cells (Brickley, Cull-Candy and Farrant; Tia et al.).

1.4.1.3 Molecular layer Interneurons (basket and stellate cells)

These interneurons are located in the molecular layer and make inhibitory synapses with Purkinje cells (Llinas and Negrello). The axons of the basket and stellate cells project upwards and align with the direction of the Purkinje cell dendrites. They use GABA as the neurotransmitter to inhibit the Purkinje cells and result in preventing the inhibitory response of the cerebellar output (da Costa and Martin).

1.4.1.4 GABAergic neurons and interneurons

GABAergic neurons produce *gamma*-Aminobutyric acid (γ-Aminobutyric acid) (GABA) as the neurotransmitter for their output. In the mammalian central nervous system, GABA is the major inhibitory neurotransmitter (Watanabe et al.). The exogenous GABA cannot cross the blood-brain barrier, therefore, it is endogenous product and synthesized by glutamate process in the brain (Kuriyama and Sze; Petroff). In addition,

the GABA that is produced by GABAergic neurons regulates the neural progenitor cells proliferation, differentiation and migration through the expression of brain-derived neurotrophic factor (BDNF) (Ganguly et al.; Obrietan, Gao and Van Den Pol).

1.4.2 Rhombic lip

The rhombic lip is a generative germinal zone that lies at the junction of the neuroepithelium of the fourth ventricle and the roof plate which can be divided into upper and lower rhombic lip (Wingate). Upper rhombic lip is formed from rhombomere 1 (r1; cerebellar primordium) and r2-8 is considered as lower rhombic lip (Wingate). The upper rhombic lip is the original source of granule cell precursors. In the cerebellum, granule cells, unipolar brush cells (UBCs), and large cerebellar nuclei neurons are considered as glutamatergic neurons which are arisen from the rhombic lip and use glutamate as the neurotransmitter.

1.4.2.1 Granule Cells

The cerebellar granule cells are one of the smallest neurons in the brain. At the same time, they are the most numerous neurons which comprise around 75%-80% of neurons in the central nervous system. The granule cells bodies are packed into a thick granule cell layer at the interior of the cerebellar cortex (Llinas and Negrello). The granule cell soma projects four to five dendrites and end in an enlargement called dendritic claw which receives excitatory input from mossy fibers and inhibitory input from Golgi cells

(Llinas and Negrello). The axon of granule cell projects to the upper layer of the cerebellar cortex where it splits into a two horizontal branched distinctive T-shape parallel fiber which passes through and synapses with the dendritic trees of Purkinje cells. The granule cells apply excitatory effects to the Purkinje cells via neurotransmitter glutamate. With the combinations of mossy fiber - the granule cells - parallel fibers to Purkinje cells, the cerebellum is able to make much finer distinctions (Marr).

During the cerebellar development, the granule cell precursors arise from the cerebellar rhombic lip and initially migrate rostrolaterally in subpial stream pathway of the cerebellar primordium to form the external germinal zone at stage 23 in human. In mouse, this process starts from embryonic day (E) 12.5 to 17 and reaches the high proliferative stages in EGZ at P7 (Machold and Fishell; Marzban et al.; Yeung et al.). In this process, SHH secreted by Purkinje cells is an important promoter of granule cell precursors proliferation (Corrales, Rocco, et al.; Haldipur et al.; Wechsler-Reya and Scott). Thus, the granule cell precursors first rapidly proliferate in EGZ and then after 24-48 hours radially move to the final destination into the granule layer and differentiate into mature granule cells (Marzban et al.; Yacubova and Komuro).

1.4.2.2 Unipolar brush cells

The unipolar brush cells play as excitatory glutamatergic interneurons that are located in cerebellar granule layer. They are named after the distinguishing dendritic ends in a brush-like structure which forms the cerebellar glomeruli with mossy fibers and

granule cell dendrites (Dino et al.; Mugnaini, Sekerková and Martina). In mouse, the unipolar brush cells are generated from E13.5 to the early postnatal period in the rhombic lip (Hevner). The unipolar brush cells migrate directly deep to the core of the developing cerebellum and reach the final destination in the granule cell layer.

1.4.2.3 Cerebellar Nuclei

The earliest glutamatergic neurons originated from the rhombic lip are projection neurons of the cerebellar nuclei (Fink et al.). The cerebellar nuclei are the only sources of output from the cerebellum. They receive axons from climbing fibers and mossy fibers and the inhibitory input from the Purkinje cells. During the development, they were born around E9–E12 in mouse (Fink et al.). The large projection cerebellar nuclei neurons migrate rostrolaterally in subpial stream pathway of the cerebellar primordium and change their direction to the destination nuclei transitory zone (NTZ).

1.4.2.4 Glutamatergic Neurons

The principal excitatory neurotransmitter in the central nervous system is glutamate that is released from the presynaptic end of glutamatergic neurons and then binds and activates the receptors on postsynaptic neurons (Freund, Katona and Piomelli). In the developing cerebellum, rhombic lip is the germinal zone that produces all glutamatergic neurons.

1.5 Sonic hedgehog

The hedgehog gene (*hh*) was first recognized in fruit-fly in 1980. The malfunction of *hh* induces a special phenotype that the embryos covered with denticles pattern that similar to spines of a hedgehog (Nusslein-Volhard and Wieschaus). Sonic hedgehog protein is encoded by *SHH* gene that is localized on chromosome 7 in human and chromosome 5 in mice. It belongs to the hedgehog family which is containing two other members; Desert hedgehog (DHH) and Indian hedgehog (IHH) (Marigo et al.). Among these three proteins, SHH is the most studied member in this family. Before SHH is secreted from the cell, it goes through many steps of translocation and modification to generate the active form of the SHH (Bumcrot, Takada and McMahon). The 45 kDa newly synthesized SHH is considered as the preproprotein. The structure of SHH preproprotein contains an N-terminal signaling region and a C-terminal region. A short signal sequence is located in the N-terminal signaling domain and used for recognized by the signal recognition particle and translocated to the endoplasmic reticulum (ER). Here the SHH undergoes an auto-cleavage process to generate a 20 kDa N-terminal signaling domain (SHH-N) and a 25 kDa C-terminal domain (SHH-C) which responsible for catalyzed by a protease but not a signaling function (Ingham, Nakano and Seger) (Fig. 1). After adding a palmitate to the SHH-N, the fully processed SHH-N is produced and responsible for the signaling activation (Pepinsky et al.).

The most prominent function of SHH is acting as a morphogen to pattern the central nervous system during the development (Litingtung and Chiang). In the cerebellum, SHH

is secreted by the Purkinje cells and plays a pivotal role in regulating the proliferation of granule cell precursors during development (Aguilar et al.; Haldipur et al.; S. J. Lee et al.; Lewis et al.).

Figure 1. The SHH preproprotein and the fully processed SHH-N

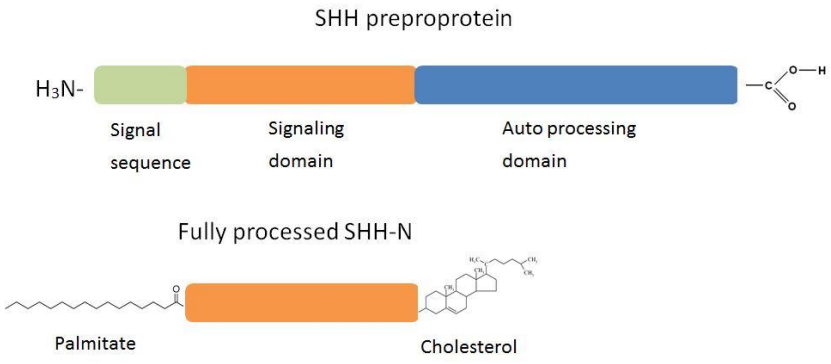

1.6 SHH signaling factors

1.6.1 Protein patched homolog 1 (PTCH1)

PTCH1 is belonged to the Patched family and encoded by *PTCH1* gene which is located on chromosome 9 in human and chromosome 13 in mouse (Johnson et al.). This protein is a 12-pass transmembrane protein and works as the receptor of SHH and suppresses the release of another protein called Smoothened (SMO) (Johnson et al.). PTCH1 functions as a control switch and regulate the SHH signaling pathway activity. A sterol sensing domain (SSD) in this protein is the key to suppress Smoothened activity (Strutt et al.). Upon PTCH1 binding with SHH, the inhibition of SMO is removed and

starts the downstream pathway.

1.6.2 Smoothened (SMO)

SMO is another important factor in SHH signaling pathway that is encoded by *SMO* gene which located on chromosome 7 in human and chromosome 6 in mouse (Ruiz-Gomez et al.). Usually, this SMO receptor is inhibited by PTCH1 when the SHH is absent. But this 7-pass transmembrane protein can initiate the downstream signaling cascade after SHH binding with the PTCH1 receptor (Taipale et al.).

1.6.3 Zinc finger protein Gli transcription factors

Gli family (glioma-associated oncogene homolog) play a very important role in SHH pathway (Corrales, Rocco, et al.; Ruiz i Altaba "Gli Proteins and Hedgehog Signaling: Development and Cancer"). The Gli transcription factors include three proteins: the activators Gli1 and Gli2 and the repressor Gli3 which are encoded by *Gli1*, *Gli2* and *Gli3* genes respectively (Ruppert et al.). The DNA binding zinc finger domains in Gli transcription factors can bind to different target genes to initiate or inhibit the transcription. These three proteins mediate the SHH signaling pathway. Gli1 is the read-out of the SHH pathway and Gli2 is responsible for active Gli target gene, such as *Gli*, *PTCH1*, *cyclins D1*and *D2*, *C-Myc, N-Myc and Wnt* (Mimeault and Batra). In contrast, Gli3 acts as the repressor of SHH signaling pathway (Jacob and Briscoe).

1.6.4 Suppressor of fused homolog (SUFU)

SUFU is a component of the SHH pathway that encoded by *SUFU* gene which is located on chromosome 10 in human and chromosome 19 in mouse (Merchant et al.). SUFU interacts directly with Gli proteins and acts as a negative regulator of SHH signaling pathway. Mutation of this gene induces multiple hereditary infundibulocystic basal cell carcinoma syndrome (Schulman et al.).

1.6.5 N-Myc proto-oncogene protein (N-Myc)

Among the Gli target genes, *MYCN* gene which is located on chromosome 2 in human and chromosome 12 in mouse that encodes the N-Myc protein which promotes proliferation of cerebellar granule cell precursors (Kenney, Cole and Rowitch; Knoepfler, Cheng and Eisenman; Ma et al.). It is shown that *MYCN* gene is associated with human neuroblastomas which is a type of tumor in the central nervous system (Schwab et al.). N-Myc is located in the cell nucleus and initiates transcription by the binding with DNA. N-Myc belongs to the Myc family which is vital for many cellular processes including proliferation, differentiation and apoptosis (Grandori et al.). Although numbers of studies indicate Myc family proteins mediate the cell fate, the detail of this pathway is still unclear.

1.7 SHH signaling pathway

When SHH is absent, SMO is inhibited by the PTCH1 receptor via removing

oxysterols from SMO. As a result, the repressor Gli3 activates and suppresses the target DNA transcription (Corcoran and Scott). When SHH binding with the PTCH1 receptor, the suppressed function by PTCH1 is removed from SMO and lead to the activity of Gli1 and Gli2 which initiate the signaling pathway downstream activity (Fig. 2).

Figure 2. SHH signaling pathway

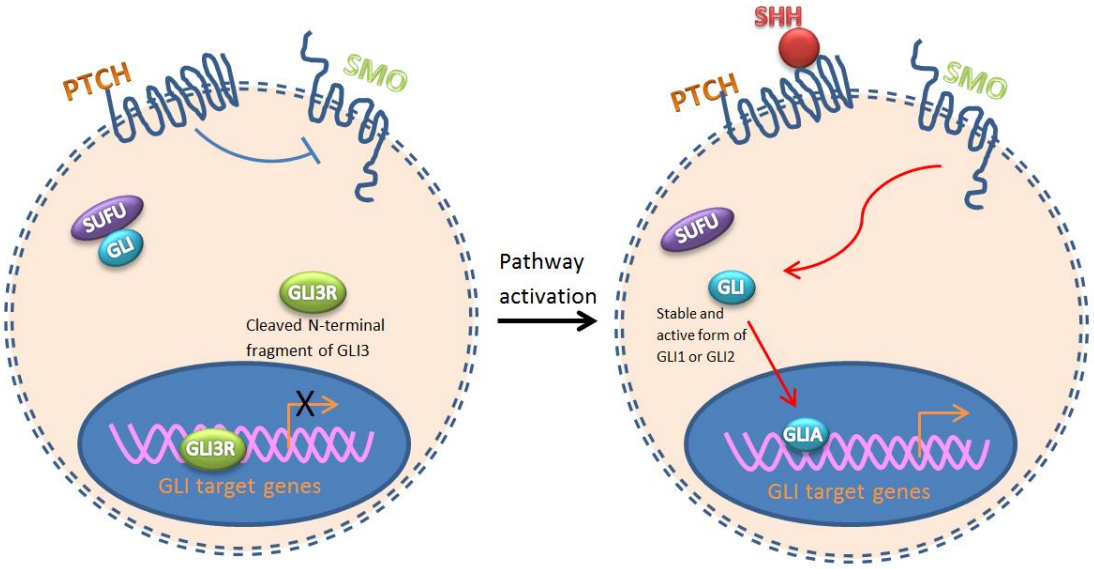

During the development, the SHH binds to the target cell and triggers the whole signaling pathway and induces the rapid proliferation of granule cell precursors in cerebellum. In cerebellum, the SHH is secreted by Purkinje cells and improve the granule cell precursors proliferation by active the whole SHH signaling pathway which is already proved by numerous studies (Dahmane and Ruiz i Altaba; Wallace; Kenney and Rowitch; Wechsler-Reya and Scott).

1.8 Lysosomal acid phosphatase 2 (Acp2) mutant mice

Lysosomal acid phosphatase 2 (Acp2) mutant mice which also called *nax* (naked-ataxia) is used in this study as an animal model. This mouse which results from a spontaneous point mutation in *Acp2* gene shows overall severe cerebellar defects with impairment of the cerebellar corticogenesis and neuronal migration (Mannan et al.). *Nax* mutant can be easily distinguished from their wt siblings via the special phenotype including growth retardation, delayed hair appearance and ataxic gait. The weight of the *nax* mutant mouse is only around 4 g while its wt sibling is around 8 g which is two times than *nax* mutant mouse at P15. The *nax* mutant mouse usually dies around P18-P26 (Bailey, Rahimi Balaei, Mannan, et al.). The size of the *nax* mutant cerebellum is also smaller and underdeveloped accompany with hypo-plastic or absent vermis. The *nax* mutant mouse also shows a severe impairment in cerebellum cytoarchitecture. It fails to form the classical three layers of the cerebellar cortex. The number of granule cells declines significantly; the Purkinje cells form the multilayer instead of monolayer and fail to form the delicate dendrites and the Bergmann glial fibers are also disorganized (Fig. 3).

This mutant phenotype resembles with Gomez Lopez Hernandez syndrome (GLHS) in human which shows the symptom that bilateral scalp alopecia, ataxia, rhombencephalosynapsis and absence of the cerebellar vermis.

Figure 3. Schematic illustration of cerebellar granule cells development from postnatal day 1 to adult in wt and *nax* mutant mouse

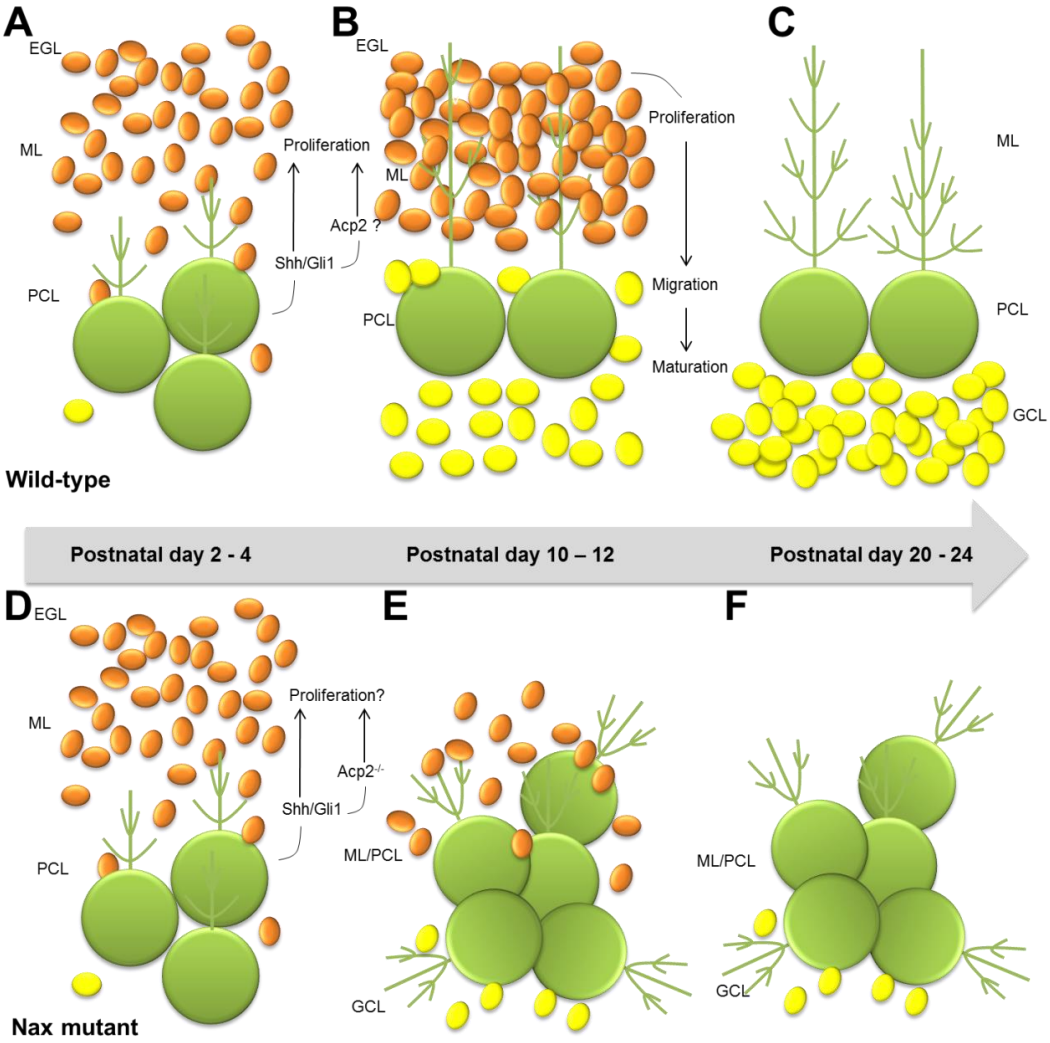

1.9 Lysosome and Lysosomal acid phosphatase 2 (LAP/Acp2)

The lysosome is membrane-bound cell organelle that is responsible for degrading and recycling macromolecules such as proteins, glycosaminoglycans, glycogen, nucleic acids, lipids as well as extracellular materials and pathogenic organisms (Lubke, Lobel and Sleat; Saftig and Klumperman). Lysosome contains different types of enzymes

including acid phosphatases, proteases, glycosidases, sulfatases and lipases (Xu and Ren; Saftig and Klumperman). Mutations in the genes for these enzymes will result in various lysosomal storage diseases, especially in the central nervous system (Platt, Boland and van der Spoel).

In human, Acp2 is an enzyme which is composed of alpha and beta subunits that are expressed in the lysosomal compartments. Acp2 alpha and beta subunits are encoded by the *Acp3* and *Acp2* genes, respectively (Ashtari et al.; Shows, Brown and Lalley). The *Acp2* gene is located on the short arm of human chromosome 11 and on chromosome 2 in the mouse. The *Acp3* gene is located on chromosome 3 in human and on chromosome 9 in the mouse. Three domains form this transmembrane protein: a single transmembrane domain, a highly glycosylated luminal domain and a carboxy-terminal cytoplasmic tail. The function of this soluble luminal hydrolase is to hydrolyze orthophosphoric monoesters into alcohol and phosphate and removes the Mannose-6-phosphate recognition marker from lysosomal proteins (Makrypidi et al.; Saftig and Klumperman; Pohlmann et al.).

It is shown that Acp2 expresses in all organs in mice, and it has a higher expression level in the testis and brain compared with other tissues. In brain tissue, Acp2 is predominately expressed in cerebellar Purkinje cells, the epithelial cells of the choroids plexus and cerebral cortical pyramidal cells. Our lab already showed the Acp2 expression during cerebellar development in C57B/6 mouse (Bailey, Rahimi Balaei, Mehdizadeh, et al.). With performing the immunohistochemistry and Western blotting in embryonic and

early postnatal mouse cerebellum, we have shown that Acp2 is expressed in the cerebellum, caudal midbrain, and fourth ventricle choroid plexus at P1 and then diffuse to different neurons. However, the Acp2 expression becomes more localized in the Purkinje cell bodies in hemispheres and posterior lobe vermis around P8. By P13, the soma and dendrite of a subset of Purkinje cells clearly show the expression of Acp2. The Western blotting analysis reveals that the Acp2 expression progressively increases in the cerebellum during development.

1.10 Proteasome

Proteasomes are protein complexes that have an important role in degrading unneeded or damaged proteins. The enzymes in this complexes that help this process are called proteases (Nassif, Cambray and Kraut). In mammals, the 26S proteasome is composed of one 20S subunit and two 19S regulatory cap subunits. In ubiquitin proteasome pathway, ubiquitin modification is an ATP-dependent process carried out by three classes of enzymes; ubiquitin-activating enzyme (E1), ubiquitin-conjugating enzyme (E2) and ubiquitin ligase (E3) (Haas et al.). The ubiquitin ligases, SCF-β-TriCP and Huwe1, regulate degradation of SHH and N-Myc respectively to balance the proliferation and differentiation in cerebellar granule cells (Zhao, Heng, et al.; Vriend, Ghavami and Marzban).

1.11 Rationale of the Study

In wt mouse, the granule cell layer contains numerous packed granule cells. However, in *nax* mutant mouse, the number of granule cells in the granule cell layer dramatically decreases and thereafter leads to the smaller cerebellum. In addition, during the development, the number of granule cell precursors is declined and trigger speculation that in *nax* mutant mouse the proliferation of the granule cell precursors is interrupted. In this study, I investigate the potential deficiency of the SHH signaling pathway and its downstream factor which may cause the impairment in the proliferation of granule cell precursors in *nax* mutant cerebellum.

Hypothesis:

The granule cells proliferation defect is associated with SHH - N-Myc pathway impairment in *nax* mutant mouse cerebellum

Specific Aim:

- To determine whether the proliferative defect of granule cell precursors causes granule cells reduction in the *nax* mutant cerebellum
- To characterize differential expression of SHH signaling molecules in the cerebellum of the *nax* mutant mouse
- To analyze whether the ubiquitin proteasome system plays a role in degradation of SHH signaling molecules in the *nax* mutant cerebellum

CHAPTER 2: MATERIALS AND METHODS

2.1 Animal maintenance

In this project, all animal procedures were based on the *Guide to the Care and Use of Experimental Animals from the Canadian Council for Animal Care (CCAC)* and University of Manitoba Animal Care Committee (ACC) and institutional regulations.

A *nax* mutant colony was established in the Genetic Model Center at the Faculty of Health Sciences, University of Manitoba after the embryos were obtained from the Institute of Human Genetics in the University Medical Center, Georg-August University, Goettingen, Germany. Then breeding mice (C57BL/6) heterozygous were used to attain the *nax* mutation. The animals were kept at room temperature and relative humidity (18–20 °C, 50%–60%) on a 12-h light-dark cycle.

2.2 Mouse Genotyping

According to the *nax* mutant mouse specific appearance, it is easy to distinguish from wt siblings, such as lacking hair of the body, smaller size and ataxia. In order to confirm the genotypes, we performed PCR by using AccuStartTM II Mouse Genotyping Kit (Quanta, Biosciences) (Bailey, Rahimi Balaei, Mannan, et al.).

2.2.1 DNA Extraction

Mouse tail or ear samples were added to a 50µl to 70µl Extraction Reagent according to the sample size. Then the samples were heated at 95°C for 30 minutes and cooled

down to room temperature. An equal volume of Stabilization Buffer was then added to the extracts. DNA extracts can be directly used to run PCR or kept at 4°C for several months.

2.2.2 Polymerase Chain reaction (PCR)

DNA extracts were used to perform PCR by AccuStartTM II Mouse Genotyping Kit (Quanta, Biosciences).

Table 1. PCR Reagents

PCR Reaction Setup Component	Volume
AccuStart II GelTrack PCR SuperMix (2X)	12.5 µl
Forward primer (Acp4F)	1 µl
Reverse primer (Acp4R)	1 µl
Nuclease-free water	5.5 µl
DNA Extract	5 µl
Final Volume (µl)	25 µl

Acp4F (5’ GCACTCTGTGCCTTCTCCAT-3’) and Acp4R (5’-CTGGGAGATTTGGGCAACTA-3’) primers were used to cut the target DNA and then amplified by PCR reaction. The PCR cycle starts with 5 cycles of a denaturation step at 95˚C for 4 min, 32 cycles of annealing step at 56˚C for 45 sec was done followed by 1 min at 72˚C extension and a final extension at 72˚C for 10 min.

2.2.3 Restriction digestion with BamHI enzyme

The total 4.16 µl reaction mixture which composed of 2.5 µl CutSmart Buffer and 1.66 µl *Bam*HI enzyme was added to each tube of 25µl PCR sample. After 2 hrs digestion with the reaction mixture at 37°C, the samples were loaded on a 2.5% agarose gel prepared in 0.5x TBE buffer with 1µg/ml ethidium bromide. The bands were visualized by Fluorchem-8900 gel imager (Alpha Innotech Corp, San Leandro, CA, USA). One 525 bp band was recognized as homozygous genotype; 320 bp and 200 bp bands were recognized as wild-type genotype; three bands of 525 bp, 320 bp and 200 bp was recognized as heterozygous genotype.

2.3 Perfusion and Cryosection

All the mice were anesthetized with 40% isoflurane, USP (Baxter Co. Mississauga, Ontario, Canada) in propylene glycol (Sigma-Aldrich Canada Co., Ontario, Canada). The mice were perfused transcardially with 15 ml 0.1 M phosphate buffer saline (pH 7.4) and 20 ml 4% paraformaldehyde (PFA) in phosphate buffer saline (PBS). The whole brains were got post-fixed with 4% PFA at least 24 hours in 4°C. Then the cerebellum was removed and processed by 10% (2 h), 20% (2 h) and 30% sucrose finally overnight at 4°C. The cerebellum was embedded and frozen in clear frozen section compound (VWR, Mississauga, Ontario, Canada) at -80°C and sectioned by cryostat with 20 µm and processed for immunohistochemistry according to our laboratory SOPs.

2.4 Immunohistochemistry

For immunohistochemistry, we use the standard protocol in our lab (Bailey, Rahimi Balaei, Mannan, et al.). The sections peroxidase immunohistochemistry was applied by washing the sections with PBS and then using 0.3% H_2O_2 for 20 min to stop the endogenous peroxidase activity. For MEF cells, 4% PFA was added to the plate to fix the cell and continued with washing process. Then, using 10% normal goat serum to block the sections incubated with the primary antibody in 0.1M PBS buffer containing 0.1% Triton X-100 overnight at room temperature. After washing with PBS, 2 hours is needed for secondary antibody incubation. Diaminobenzidine (DAB, 0.5 mg/ml) was used as the chromogen to show the reaction signal. Then the sections were dehydrated through an alcohol series (70%, 95%, and 100%) and cleared with xylene and finally covered with coverslip by mounting medium.

2.5 Immunofluorescence

The difference between double staining and peroxidase immunohistochemistry were incubated with several different primary antibodies at room temperature overnight and the secondary antibodies are Alexa Fluor 488 goat anti-mouse or anti-rabbit IgG and Alexa Fluor 594 goat anti-rabbit or anti-mouse IgG. The sections were covered with Fluorsave. For autofluorescence control, just remove the step for primary antibody and obtain other steps same with regular double staining.

- *Primary antibodies used in immunohistochemistry and immunofluorescence*

- Anti-NeuN Rabbit Polyclonal, Millipore Sigma, 1:1000
- Anti-Pax6 Mouse Monoclonal, Developmental Studies Hybridoma Bank, 1:25
- Anti-Sonic hedgehog Rabbit Polyclonal, Millipore Sigma, 1:200
- Anti-Calbindin D-28K Mouse Monoclonal, Swant, 1:1000
- Anti-Gli1 Rabbit Polyclonal, Abcam, 1:500
- Anti-N-Myc Mouse Monoclonal, Millipore Sigma, 1:25
- Anti-Proteasome 20S alpha + beta rabbit Polyclonal, Abcam, 1:400

➢ *Secondary antibodies used in immunohistochemistry and immunofluorescence*

- Goat anti-mouse IgG, HRP conjugate, Millipore Sigma, 1:500
- Goat anti-rabbit IgG, HRP conjugate, Millipore Sigma, 1:500
- Alexa Fluor 488 goat anti-mouse IgG, Thermo Fisher, 1:1000
- Alexa Fluor 488 goat anti-rabbit IgG, Thermo Fisher, 1:1000
- Alexa Fluor 594 goat anti-mouse IgG, Thermo Fisher, 1:1000
- Alexa Fluor 594 goat anti-rabbit IgG, Thermo Fisher, 1:1000

2.6 Western blot

The cerebellum samples were collected at different age (P1, P5, P7, P10, P12, P15 and P19) of *nax* mutant and wt sibling mouse or the MEF cells and then put the sample in appropriate amount lysis buffer according to the tissue size which containing protease inhibitor cocktail (Life Science, cat# M250) and phosphatase inhibitor (Sigma Aldrich, cat# P5726). After sonication of the sample, the protein concentration measured by using

BCA protein assay kit (Bio-Rad cat#5000121). The protein sample suspended in loading buffer (Tris-HCl 60mM, glycerol 25%, SDS 2%, mercaptoethanol (ME) 14.4Mm, bromophenol blue 0.1%, H2O) and separated by sodium dodecyl sulfate polyacrylamide gel electrophoresis. Based on the molecular weight of the protein, a 6-15% polyacrylamide gel was chosen to perform the electrophoresis. 15 µl of each sample was loaded and 10 µl precision plus protein was used as marker standard (Thermo Fischer Scientific, ON, Canada). Then the protein was transferred to a polyvinylidene fluoride membrane. First, block the membrane with 5% milk and incubate it with primary antibody in 1x TBST (Tris-buffered saline/0.01% tween 20) overnight at 4°C, then wash with 1xTBST 20 min for 3 times and incubate with secondary antibody in 1x TBST for 2 hours. Membranes were washed 20 min 3 times and the immunoreactive bands were visualized by electrochemiluminescence (ECL) (Pierce, ON, Canada). The data was analyzed by AlphaEase software and the band was measured and normalized to the β-Actin.

- *Primary antibodies used in Western blot*
  - Anti-Sonic hedgehog Rabbit Polyclonal, Cell Signaling, 1:500
  - Anti-N-Myc Mouse Monoclonal, Millipore Sigma, 1:500
  - Anti-Proteasome 20S alpha + beta rabbit Polyclonal, Abcam, 1:1000
  - Anti- Beta(β)- Actin Monoclonal, Millipore Sigma, 1:5000
- *Secondary antibodies used in Western blot*
  - Goat anti-mouse IgG, HRP conjugate, Millipore Sigma, 1:5000

- Goat anti-rabbit IgG, HRP conjugate, Millipore Sigma, 1:5000

2.7 Cell counting

The cerebellar granule cells in granule layer and granule cell precursors in the external germinal zone were counted using ImageJ software. Three slides were counted for wt and *nax* mutant mouse.

2.8 Mouse Embryonic Fibroblasts (MEFs) culture

Sacrifice a heterozygous pregnant mouse and embryos were dissected and removed the head and red organs. The tail was used to perform PCR for distinguishing the genotype. The body was first ground and then digested with 0.25% Trypsin/EDTA (Gibco, Cat#15090-046). Discharge the supernatant after centrifuging the sample. The pellet was re-suspended and added on a coated plate (0.1% Gelatin solution) and incubated with MEF medium (10% fetal bovine serum, 1% 200 mM L-glutamine and 1% Penicillin-streptomycin in high glucose DMEM) at 37°C 5% CO_2 until confluent. The cells were frozen and stored in liquid nitrogen. Then the cells can be collected and used for experiments such as immunostaining, Western blotting, and manipulating as required.

2.9 26S Proteasome activity assay

26S proteasome consists of two parts, 19S proteasome which is the regulatory part and 20S proteasome which is the site where proteolysis of protein occurs (Vriend,

Ghavami and Marzban). For measuring 19S proteasome activity, seed cells in a 96-well plate with a density of 10^5-10^6 cells/well and incubate overnight at 37°C 5% CO_2. After centrifuging the plate and aspirating the culture medium, add the 19S Proteasome Assay Buffer and centrifuge the plate again. Discard the supernatant and add the Proteasome Lysis Buffer (Cayman chemical Item No. 10011098) and incubate with gentle shaking for 30min at room temperature. Transfer 90 µl supernatant to a black 96-well plate after the centrifuging and add 10 µl 19S Assay Buffer. After adding the Ubiquitin-Rhodamine 110 (Boston Biochem Item Cat#U-555) Substrate Solution, the fluorescent intensity can be read over 1 hour (excitation = 485 nm; emission = 535 nm). For measuring 20S proteasome activity, seed cells in a 96-well plate with a density of 10^5-10^6 cells/well and incubate overnight at 37°C 5% CO_2. After centrifuging the plate and aspirating the culture medium, add the 20S Proteasome Assay Buffer (Cayman chemical Item No. 10011097) and centrifuge the plate again. Discard the supernatant and add the Proteasome Lysis Buffer (Cayman chemical Item No. 10011098) and incubate with gentle shaking for 30min at room temperature. Transfer 90 µl supernatant to a black 96-well plate after the centrifuging and add 10 µl SUC-LLVY-AMC substrate (Cayman chemical Item No. 10011095). The fluorescent intensity can be read after incubating the plate 1 hour in dark (excitation = 360 nm; emission = 480 nm).

2.10 Imaging

Zeiss Axio Imager M2 microscope (Zeiss, Toronto, ON, Canada) was used to capture

bright field image and analyzed with Zeiss Microscope Software (Zen Image Analyses software; Zeiss, Toronto, ON, Canada). Fluorescent images were captured by Zeiss Z1 and Z2 Imager, Zeiss LSM 700 confocal microscope (Zeiss, Toronto, ON, Canada). In order to edit and montage the image, Adobe Photoshop CS5 was used to edit, crop and finalize the images.

2.11 Statistical analysis

GraphPad Prism 6 was used to analyze the difference by one-way/two-way analysis of variance (ANOVA) for more than two groups and student t-test for two groups. The Significant difference was set at $P<0.05$. In the figure, P* <0. 05, P**<0.01. All the experiments were repeated 3 times.

CHAPTER 3: RESULT

Aim #1: To determine whether the proliferative defect of granule cell precursors causes granule cells reduction in the *nax* mutant cerebellum

3.1 *The number of cerebellar granule cells is significantly decreased in nax mutant mouse compared with wild-type sibling mouse*

According to our previous study and data, we found that the *nax* mutant mouse is smaller in size and shows an overall impairment of the cerebellar cortex and nuclei (Bailey, Rahimi Balaei, Mehdizadeh, et al.). The cerebellar well-organized three-layer cortex is disrupted in *nax* mutant with a significant decrease in granule cells, over-migration of Purkinje cells (Bailey, Rahimi Balaei, Mannan, et al.), and disorganized Bergmann glial fibers.

In order to understand the developmental differences of the cerebellar granule cells in wt and *nax* mutant mouse, we used NeuN antibody to specifically label mature granule cells. At P13, NeuN immunostaining shows a large number of granule cells which is packed granule cell layer in wt mouse cerebellum (Fig. 4, A-C), while in *nax* mutant cerebellum there is a marked decrease of the granule cells (Fig. 4, D-F). The number of cerebellar granule cells is significantly reduced both in cerebellar vermis and hemisphere in *nax* mutant mouse, which is around 20% of the wt sibling mouse (Fig. 4, H).

The reduction of granule cells could be due to a defect in proliferation or migration deficiency from EGZ to granule cell layer (Mallet et al.). At P13, the number of the mature granule cells in *nax* mutant cerebellum is markedly reduced (Fig. 4). To explore

whether the granule cells proliferative activity in EGZ is impaired, the Paired box protein 6 (Pax6) immunostaining is used at P6 wt and *nax* mutant mouse to display the granule cell precursors. It is revealed that the number of granule cell precursors clearly decreases in EGZ of the *nax* cerebellum (Fig. 5, A-B) and is only about 20% compared with wt sibling mouse (Fig. 5, C). In order to further confirm this observation and identify granule cell precursors in EGZ in relation to Purkinje cells development, we applied double staining with Pax6 and Calcium-binding protein (CaBP) which is a marker for Purkinje cells in the cerebellum. At P8 wt mouse, it shows a thick EGZ with granule cells precursors in medial and lateral cerebellum (Fig. 5, D, F-G). In contrast, the *nax* mutant cerebellum displays a reduced number of granule cell precursors in the EGZ that is apparently absent medially (putative vermis) and thin in lateral cerebellum (Fig. 5, E, H-I).

Figure 4. The number of cerebellar granule cells is significantly decreased in *nax* mutant mouse compared with wt sibling mouse

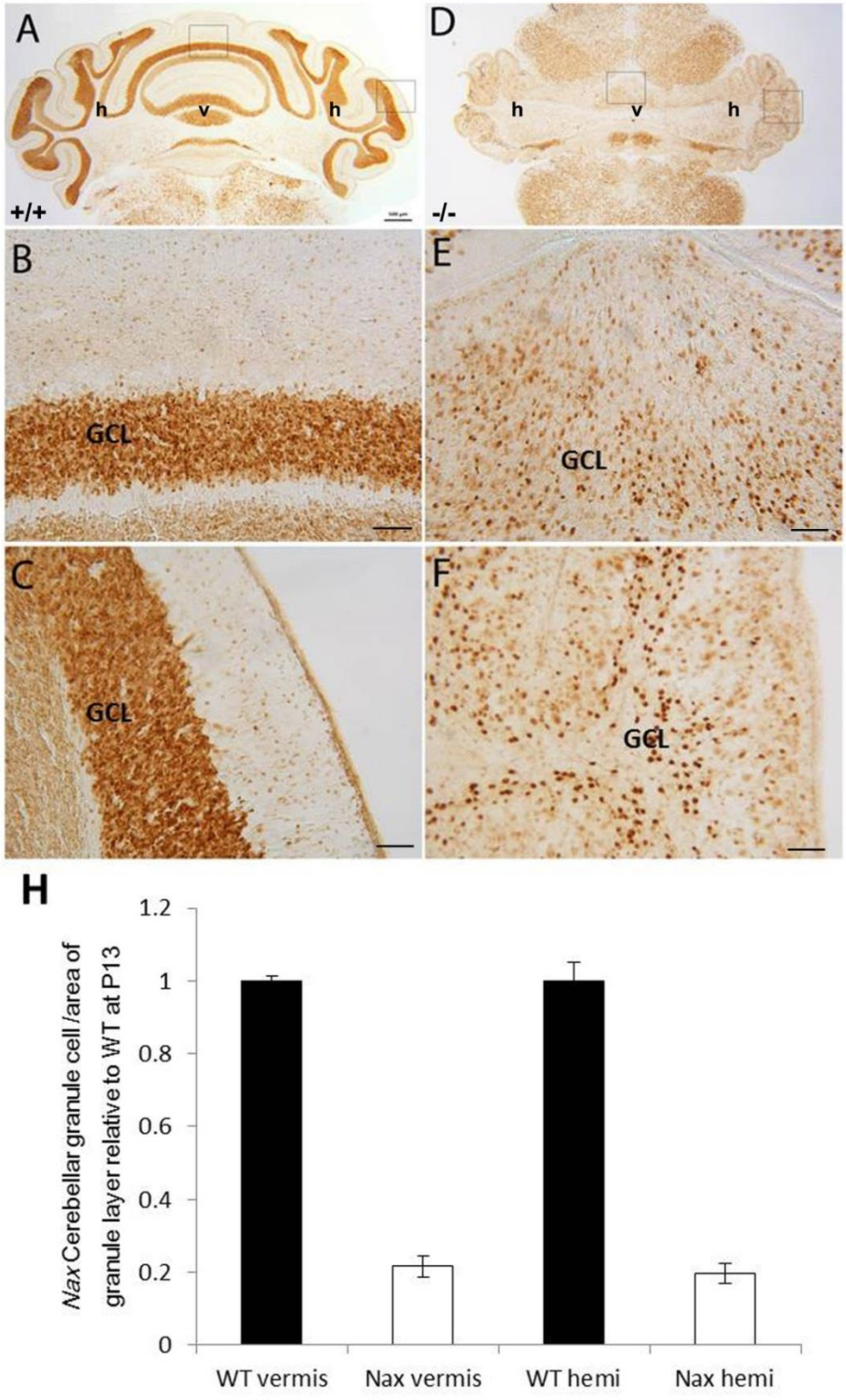

(A) Frontal section of P13 wt mouse cerebellum immunostained with NeuN reveals a large number of granule cells in granule cell layer (GCL). **(D)** Frontal section of P13 *nax* mouse cerebellum immunostained with NeuN shows the cerebellum size is smaller and the lobules are underdeveloped. The number of cerebellar granule cells is significantly decreased. **(B, C)** the higher magnification show medially **(B)** and laterally **(C)** of wt cerebellum **(A)**. **(E, F)** the higher magnification show medially **(E)** and laterally **(F)** of *nax* cerebellum **(D)**. **(H)** Cell counting of the frontal sections of P13 samples shows a significant difference in the number of granule cell in wt and *nax* **(C)**. The bars represent the average cell counts at P13 wt and *nax* siblings (wt; n=3 and *nax*; n=3) and show that granule cells are only around 20% of wt both at cerebellar vermis and hemisphere. The data in the bar graph are presented as the mean ± SEM, and statistical analysis was performed using unpaired t-test ($P<0.05$). GCL, granule cell layer; h, hemisphere; v, vermis. Scale bar = 500 μm in **(A, D)** and 100 μm in **(B-F)**.

Figure 5. The proliferative activity of the cerebellar granule cells is impaired in *nax* mutant mouse cerebellum

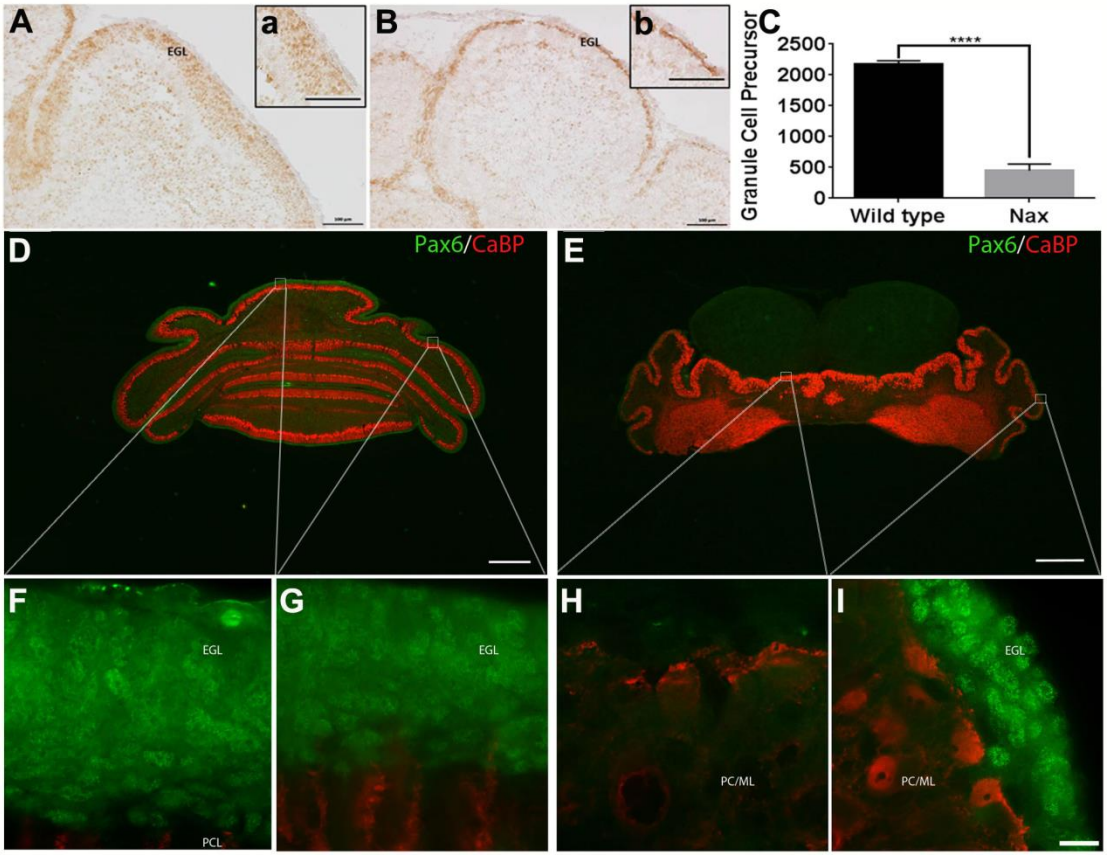

(A) Sagittal section of P6 wt mouse cerebellum immunostained with Pax6 shows granule cell precursors in the external germinal zone (EGZ) and shows in higher magnification **(a)**. **(B)** Sagittal section of P6 *nax* mouse cerebellum immunostained with Pax6 displays the number of granule cell precursors is significantly decreased and shows in higher magnification in **(b)**. **(C)** Cell counting of the sagittal sections of P6 cerebellum shows a significant difference in the number of granule cell precursors during early postnatal age in wt and *nax*. The bars represent the average cell counts at P6 wt and *nax* siblings (wt; n=3 and *nax*; n=3) and show that granule cell precursors are only around 20% of wt. The

data in the bar graph are presented as the mean ± SEM, and statistical analysis was performed using unpaired t-test ($P<0.05$). **(D-E)** Frontal sections of wt **(D)** and *nax* **(E)** cerebellum at P8 immunostained with Pax6 (green) and CaBP (red). **(D)** In the wt mouse, a thick external germinal zone (EGZ) occurred medially **(F)** and laterally **(G)** in the wt cerebellum. **(E)** In the *nax* mutant, a reduced number of proliferating granule cells occurred in the EGZ, in which appeared absent medially **(H)** and with a thin EGZ occurred in the *nax* mutant laterally **(I)**. EGZ, external germinal zone; ML, molecular layer; PCL, Purkinje cell layer. Scale bar = 500 μm in **(A, B)** and 100 μm in **(a, b)** and 1000 μm in **(D, E)** and 20 μm in **(I)**.

3.2 *Bergmann glial cell developmental defect in nax mutant cerebellum*

During development, the Bergmann glial cells are associated with cerebellar corticogenesis and development and migration of the granule cells (Yamada and Watanabe; D'Arca et al.). To determine whether granule cell maldevelopment is associated with Bergmann glial cells in *nax* cerebellum, we used Glial fibrillary acidic protein (GFAP) for immunohistochemistry in wt and *nax* cerebellum. In wt, the Bergmann glial fibers project straight through the molecular layer to the subapial surface and terminate as endfeet in both vermis and hemisphere (Fig. 6, A-C). The section from *nax* mutant cerebellum staining with GFAP shows that the Bergmann glial cell morphological changes in the developing cerebellar cortex and are not appear aligned in putative Purkinje cells layer and glial fibers are disorganized in both vermis and

hemisphere (Fig. 6, E, F).

Double staining with Pax6 and GFAP shows Bergmann glial fibers project straight and perpendicular to the pial surface pass through the molecular layer and the thick layer of EGZ (Fig. 7, A-C). In *nax* mutant, the Bergmann glial fibers appear severely disorganized in an area with lack of granule cell precursor in EGZ particularly in vermis (Fig. 7, E). However, in the hemisphere, the Bergmann glial fibers appear more organized compared to *nax* cerebellar vermis in which a thin layer of granule cell precursors present (Fig. 7, F).

Figure 6. Bergmann glial cell is disorganized in *nax* cerebellum at P13

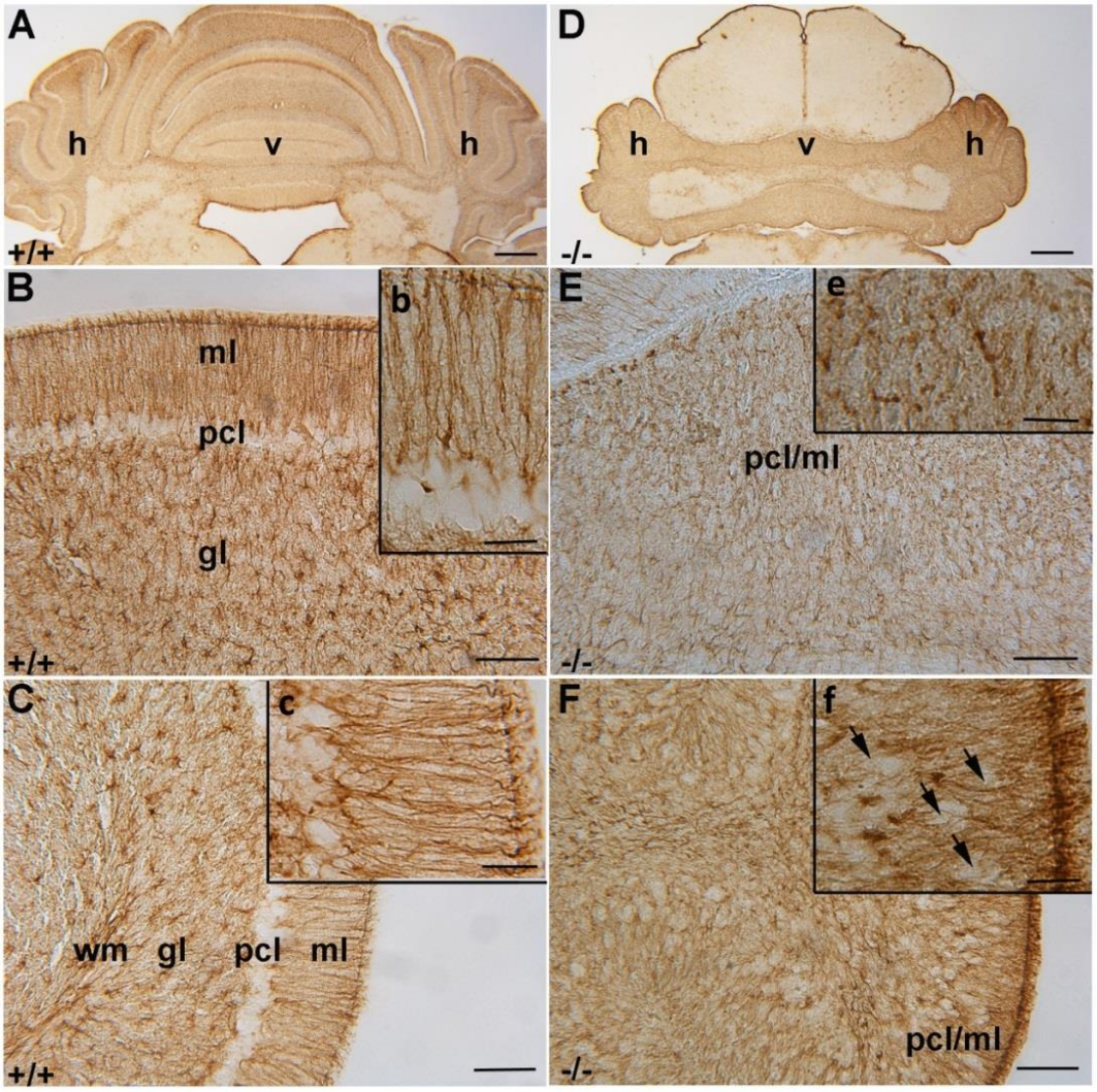

(A-C) Frontal sections of the wt sibling cerebellum are immunostained with GFAP and show the astrocyte and Bergmann glial cell immunoreactivity. Bergmann glial cell bodies align with PC layer and their fibers project straight into the molecular layer in the vermis **(B)** and hemisphere **(C)** areas of the cerebellum in wt mice. (b-c) show the high magnification of **(B-C)**. **(D-F)** Frontal sections of the *nax* cerebellum are immunostained for GFAP and show astrocyte and Bergmann glial cell immunoreactivity. Bergmann glial

cell bodies don't appear aligned in a straight line and fibers appear less organized, with some projecting to the pial surface in vermis **(E)**. Bergmann glial cells appear more organized in the hemisphere of the *nax* cerebellum **(F)** which located in between the ectopic Purkinje cell in the molecular layer (arrow). gl, granular layer; h, hemisphere; ml, molecular layer; pcl, Purkinje cell layer; v, vermis; wm, white matter. Scale bar = 500 μm in **(A, D)** and 100 μm in **(B-F)** and 50 μm in **(b-f)**.

Figure 7. Bergmann glial cell is disorganized in *nax* cerebellum at P10

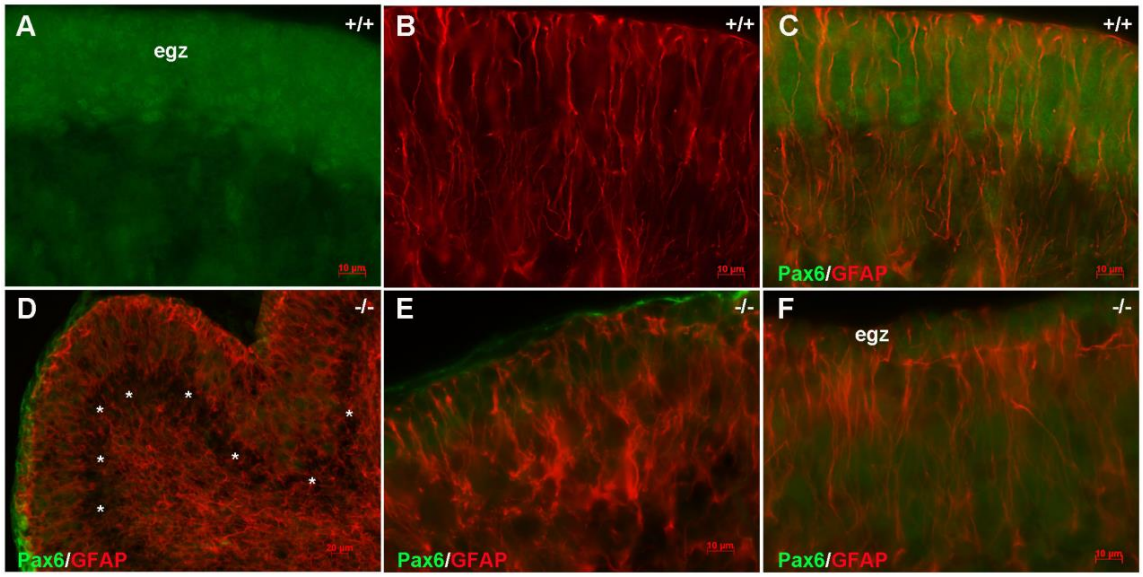

(A-C) Frontal sections of the wt sibling cerebellum are immunostained with GFAP (red) and Pax6 (green) at P10 shows Bergmann glial cell bodies align with Purkinje cell layer and their fibers project straight into the granule cell precursors and end to the subpial surface as endfeet in wt mice cerebellum. **(D-F)** Frontal sections of the *nax* cerebellum are immunostained with GFAP (red) and Pax6 (green) at P10 shows Bergmann glial cell

appear disorganized **(E)** with lack of granule cell precursors. Asterisk indicates the location of the PC somas in **(D)**. Bergmann glial cells appear more organized in the hemisphere of the *nax* cerebellum **(F)** with a thin layer of granule cell precursor in EGZ. egz, external germinal zone. Scale bar = 10 μm in **(A-C, E-F)** and 20 μm in **(D)**.

Aim #2: To characterize differential expression of SHH signaling molecules in the cerebellum of the *nax* mutant mouse

3.3 *SHH signaling pathway involved in cerebellar granule cells development and proliferation in wt and nax mutant mouse*

SHH signaling pathway is an important regulator of granule cells precursor proliferation during cerebellar development (Corrales, Rocco, et al.; Haldipur et al.; Wechsler-Reya and Scott). In order to understand if the SHH pathway is impaired in granule cell precursors proliferation, SHH immunostaining (Fig. 8) and Western blot analysis (Fig. 9) were performed in wt and *nax* mutant cerebellum. Cerebellar section immunostained with SHH antibody at P5 and P13 in wt and *nax* mutant mouse shows the similar distribution of the SHH in Purkinje cell in both groups (Fig. 8, A-D).

Figure 8. SHH is expressed by cerebellar Purkinje cells in wt and *nax* mutant mouse

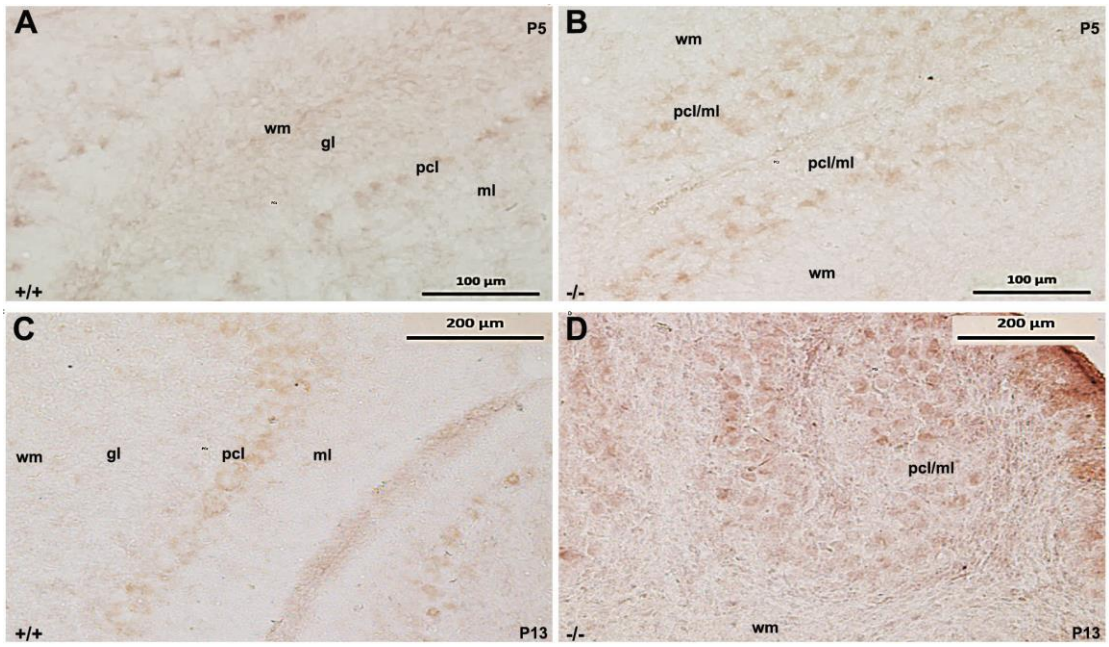

(A, B) Sagittal section of P5 wt and *nax* mutant mouse cerebellum immunostained with SHH show the expression of SHH is localized in Purkinje cells in both wt and *nax* sibling cerebellum. **(C, D)** Sagittal section of P13 wt and *nax* mutant mouse cerebellum immunostained with SHH show the similar expression as P5. gl, granule cell layer; ml, molecular layer; pcl, Purkinje cell layer wm, white matter. Scale bar = 100 µm in **(A, B)** and 200 µm in **(C, D)**.

***3.3.1** SHH expression shows a similar pattern in wt and nax mutant mouse cerebellum*

To determine the SHH expression pattern, Western blot analysis was applied at P1, P5, P7, P10, P12, P15 and P19 in wt and *nax* mutant mouse cerebellum. The SHH expression up-regulates from P1 to P5 and reaches the peak then down-regulates from P10 in wt mouse (Fig. 9). However, in the *nax* mutant mouse cerebellum, the SHH

expression has a slight difference. The SHH reaches the peak at P7 and then down-regulates until P12 followed by a small increase at P15 and P19 (Fig. 9). Overall, the expression of SHH is lower in *nax* mutant mouse but the difference is not significant (Fig. 9).

Figure 9. SHH expression shows a similar pattern in wt and *nax* mutant mouse cerebellum

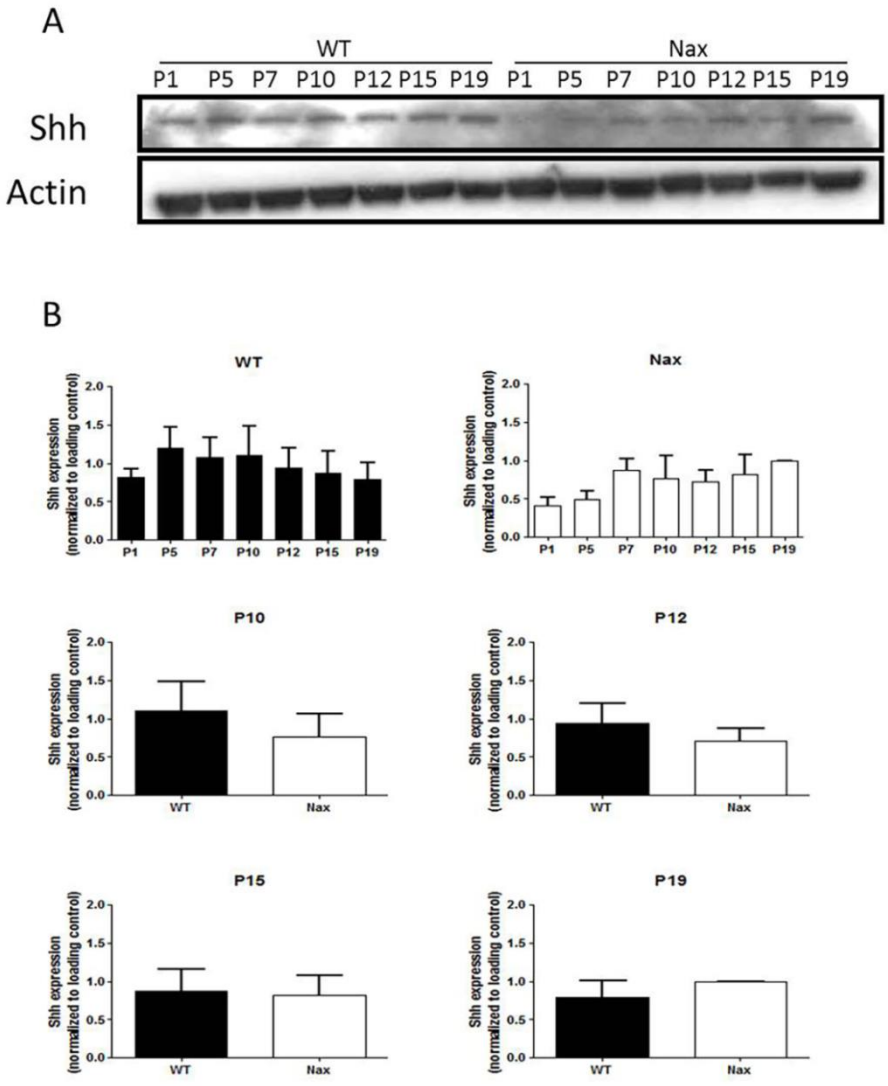

(A, B) Western blot analysis of SHH expression in wt and *nax* mutant mouse cerebellum at P1, P5, P7, P10, P12, P15 and P19 reveals similar pattern but a slightly lower expression in *nax* mutant (wt: n=3 and *nax*: n=3). The actin shows the consistent loading in all cerebellar samples. The data in the bar graph are presented as the mean of three independent experiments ± SEM, and statistical analysis was performed using one-way ANOVA.

3.4 *Gli1 acts as an important mediator of SHH pathway and expresses in Pcs and gcps both in wt and nax mutant mouse*

Gli1 is a readout of positive SHH signaling pathway and is involved in cell fate determination, proliferation and patterning in many cell types during embryonic development (Ruiz i Altaba "Gli Proteins Encode Context-Dependent Positive and Negative Functions: Implications for Development and Disease"). Immunostaining with Gli1 antibody at P5 cerebellum is performed to determine whether there is any change in Gli1 expression in *nax* mutant cerebellum in comparison to wt sibling. The result shows the almost similar pattern of the Gli1 expression and distribution which is localized in granule cell precursors and Purkinje cells in wt and *nax* mutant mouse cerebellar cortex (Fig. 10).

Figure 10. Gli1 is expressed in Pcs and gcps in wt and *nax* mutant mouse cerebellum at P5

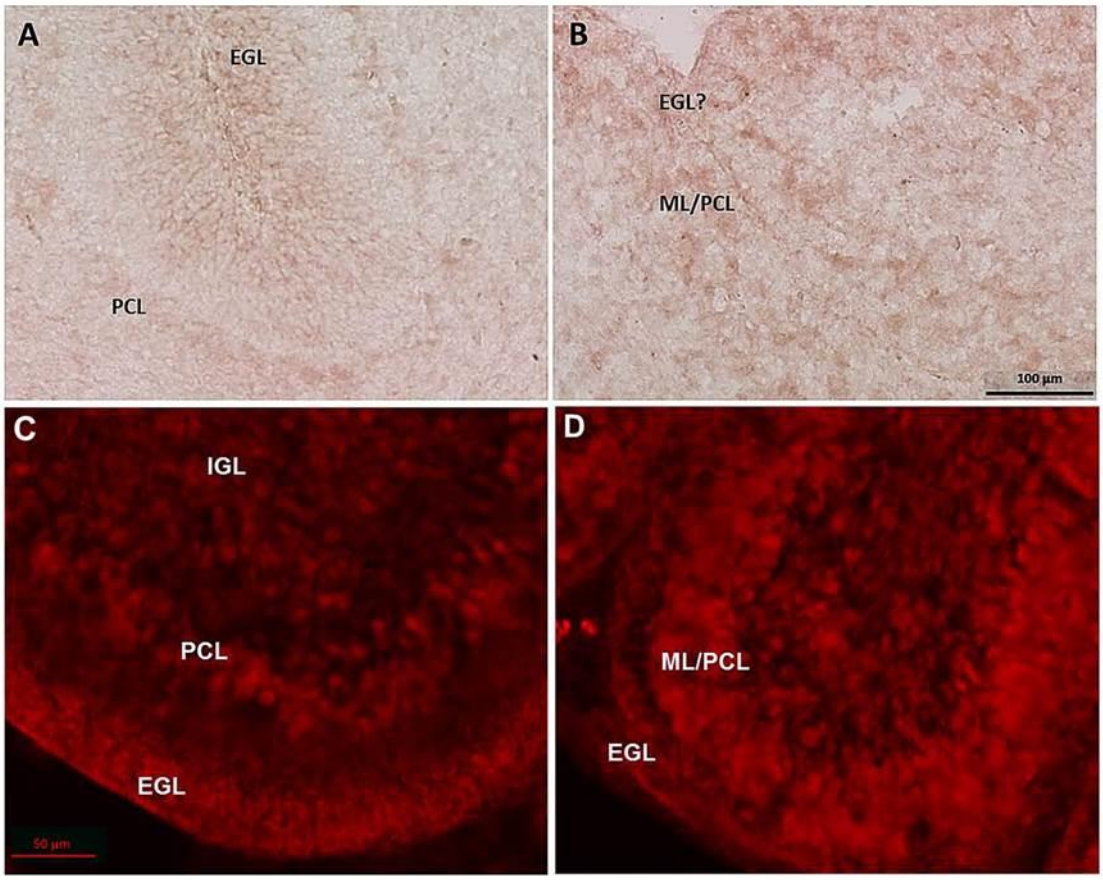

(A, B) Sagittal section of P5 wt and *nax* mutant mouse cerebellum immunoperoxidase stained with Gli1 shows almost the same expression in cerebellar Purkinje cells and granule cell precursors and granule cells. **(C-D)** Sagittal sections of wt and *nax* mutant cerebellum at P5 are performed with immunofluorescence staining with Gli1. EGL, external germinal zone; IGL, internal granule layer; ML, molecular layer; PCL, Purkinje cell layer. Scale bar = 100 µm in **(A, B)** and 50 µm in **(C-D)**.

3.5 *N-Myc expression pattern in granule cell precursors in wt and nax mutant mouse cerebellum*

N-Myc, a direct downstream target of SHH pathway, is highly expressed in embryonic brain and plays a vital role in development, especially for cerebellar granule cell precursors proliferation (Hatton et al.; Kenney, Cole and Rowitch; Knoepfler, Cheng and Eisenman). To determine whether the N-Myc expression is impaired in *nax* mutant cerebellum, immunostaining with N-Myc antibody is performed in wt and *nax* mutant mouse at P5 and P12. It reveals that N-Myc is expressed by granule cell precursors in *nax* mutant mouse at P5 (Fig. 11, A-B) and P12 (Fig. 11, C-D) which is comparable with expression pattern in wt after birth. However, double staining with N-Myc and CaBP at P5 (Fig. 12) and the sagittal sections of P12 (Fig. 11, C-D) show the lower expression of N-Myc in *nax* mutant mouse cerebellum when compared with the wt sibling cerebellum.

Figure 11. N-Myc is expressed by granule cell precursors in wt and *nax* mutant mouse at P5 and P12

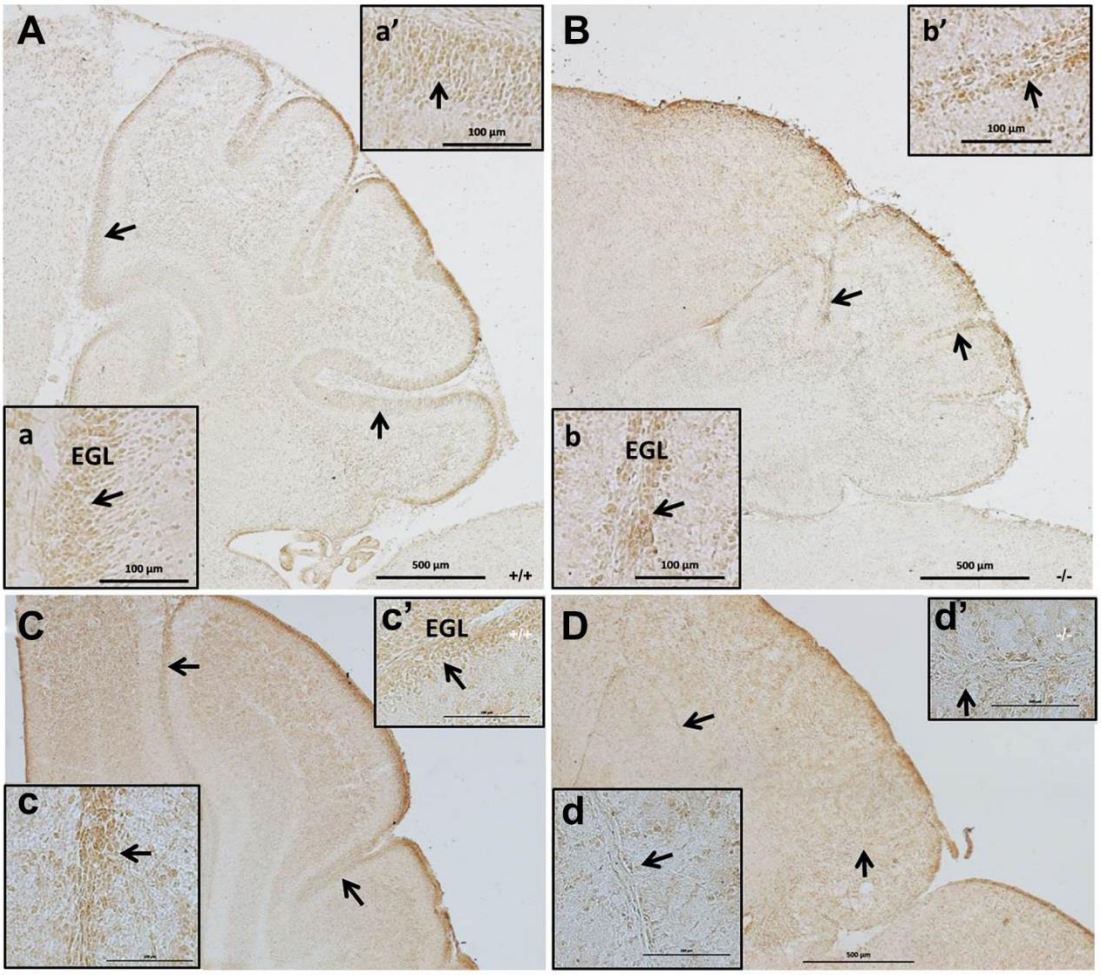

(A, B) Sagittal section of P5 wt and *nax* mutant mouse cerebellum immunostained with N-Myc shows expression in granule cell precursors. **(a)** Anterior lobe and **(a')** posterior lobe are the higher magnification of wt cerebellum **(A)**. **(b)** Anterior lobe and **(b')** posterior lobe show higher magnification of *nax* cerebellum **(B)**. **(C-D)** Sagittal section of P12 *nax* mutant mouse cerebellum **(D)** immunostained with N-Myc shows lower expression in granule cell precursors compared with wt sibling **(C)**. **(c)** Anterior lobe and **(c')** posterior lobe are the higher magnification of wt cerebellum **(C)**. **(d)** Anterior lobe

and **(d')** posterior lobe show higher magnification of *nax* cerebellum **(D)**. EGZ, external germinal zone. Scale bar = 500 μm in **(A, B)** and 100 μm in **(a-b')** 500 μm in **(C, D)** and 100 μm in **(c-d')**.

Figure 12. N-Myc and CaBP double immunostaining at P5 shows lower expression in *nax* mouse while compared with wt sibling

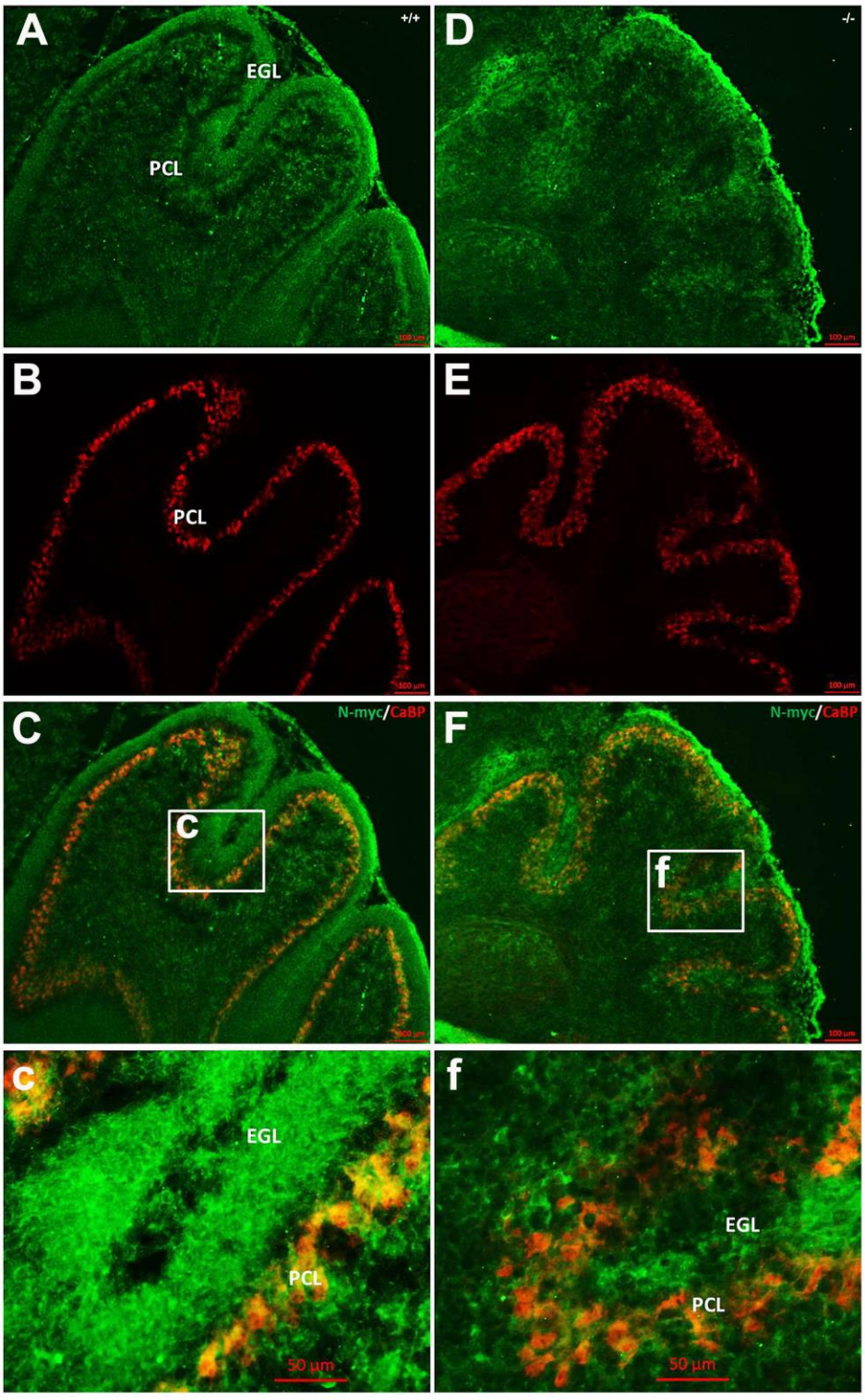

(A-F) Sagittal sections of wt **(A-C)** and *nax* **(D-F)** mutant cerebellum at P5 were performed with immunofluorescence histochemistry with N-Myc (green) and CaBP (red). **(c)** is the higher magnification of wt cerebellum **(C)** and **(f)** shows higher magnification of *nax* cerebellum **(F)**. EGZ, external germinal zone; PCL, Purkinje cell layer. Scale bar = 100 μm in **(A-C, D-F)** and 50 μm in **(c, f)**.

3.5.1 *N-Myc expression pattern is downregulated in nax mutant mouse*

Western blot analysis was performed to confirm the protein identification and alteration in N-Myc expression in *nax* mutant mouse cerebellum in comparison with wt sibling from P1 to P19. The N-Myc expression up-regulates from P1 to P10 and reaches the peak then down-regulates from P10 in wt mouse cerebellum (Fig. 13). However, in the *nax* mutant mouse cerebellum, the N-Myc expression is generally impaired. The N-Myc reaches the peak at P7 and then down-regulates until P19 (Fig. 13). Overall, the expression of N-Myc is striking decreased at P10 which is the most active stage for cerebellar granule cell precursors proliferation and P15 in *nax* mutant mouse cerebellum (Fig. 13).

Figure 13. N-Myc shows a lower expression in *nax* mutant mouse at P10 and P15

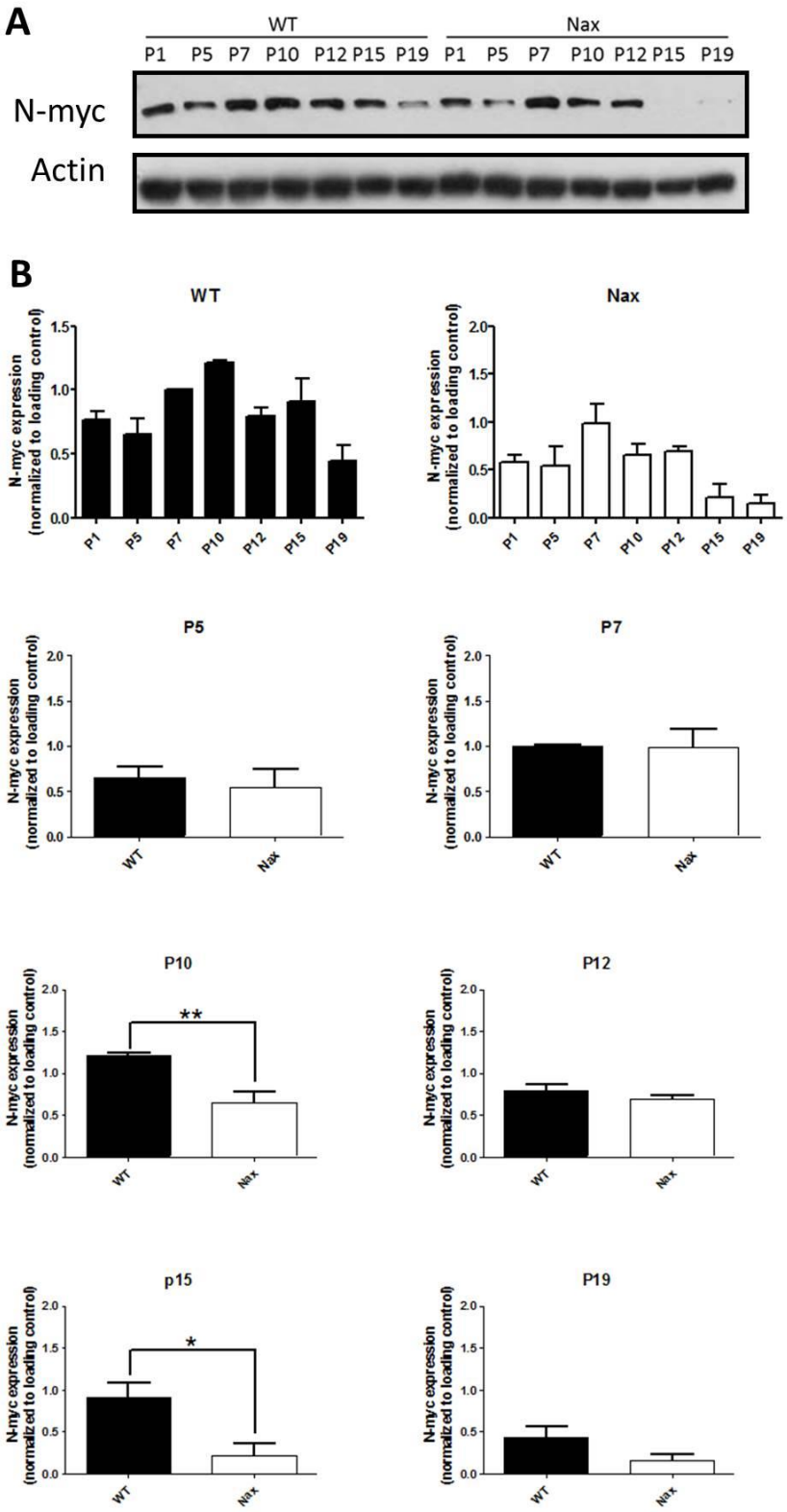

(A) Western blot analysis of N-Myc expression in wt and *nax* mutant mouse cerebellum at P1, P5, P7, P10, P12, P15 and P19 reveals an overall lower expression in *nax* mutant (wt: n=3 and *nax*: n=3). The actin shows the consistent loading in all cerebellar samples. **(B)** Western blot analysis of N-myc expression comparison for different postnatal days between wt and *nax* mutant mouse and shows a significant decrease in P10 and P15. The data in the bar graph are presented as the mean of three independent experiments ± SEM, and statistical analysis was performed using one-way ANOVA (P* <0. 05, P**<0.01).

3.6 *MEF^{nax} express lower amount of the N-Myc compared with MEF^{wt}*

In order to further explore the N-Myc expression impairment in *nax* mutant mouse; we used mouse embryonic fibroblasts (MEFs) as a tool to investigate the synthesis and degradation of N-Myc in *nax* mouse. N-Myc immunostaining shows a weak signal in MEF^{nax} compare with MEF^{wt} (Fig. 14, A-F). The Western blot analysis confirms the lower expression of N-Myc in MEF^{nax} which is around 50% of MEF^{wt} (Fig. 14, G, H).

Figure 14. MEF^{nax} express lower amount of the N-Myc compared with MEF^{wt}

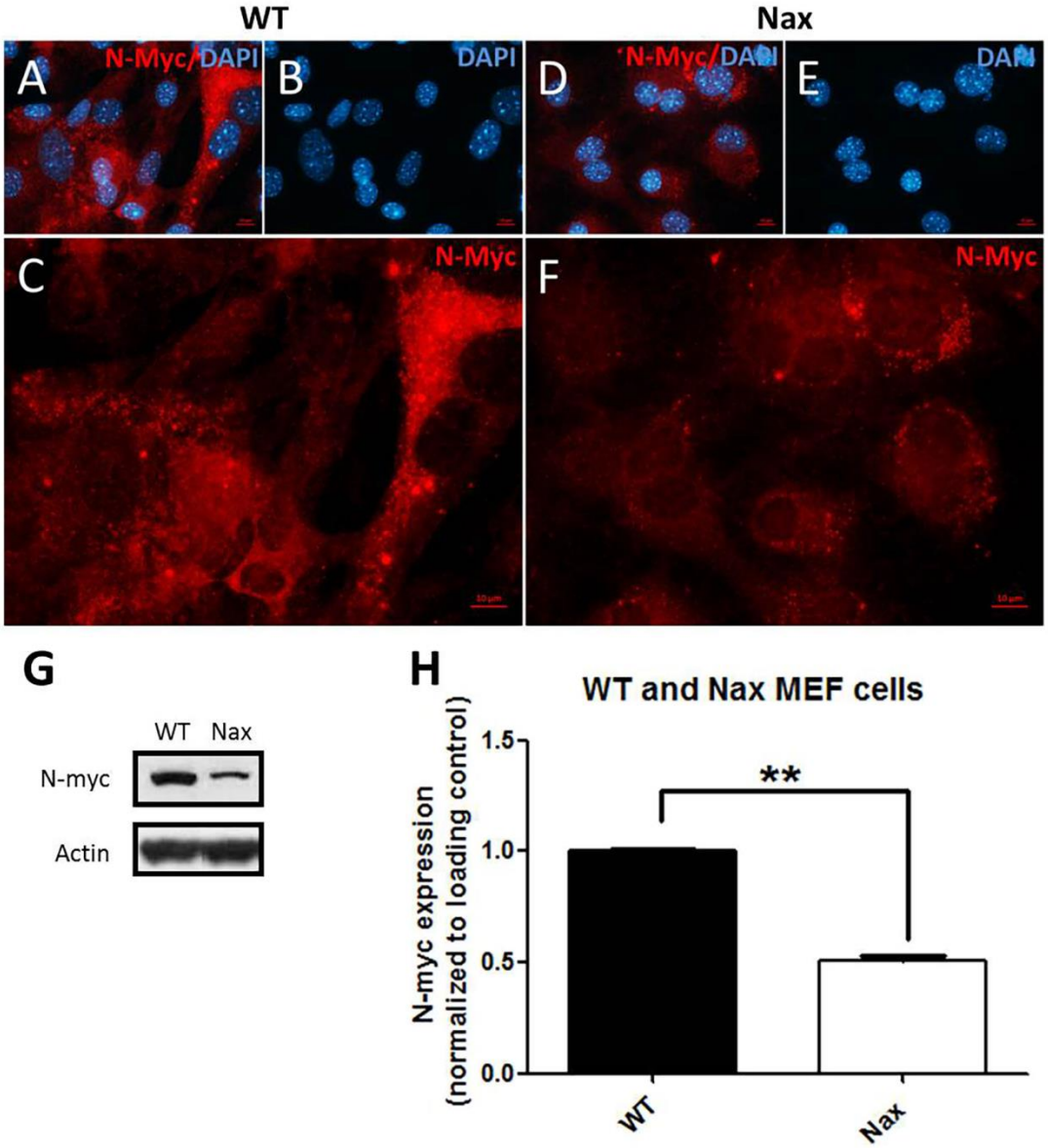

(A-C) Immunofluorescence staining of the MEF^{wt} with N-Myc (red) and DAPI (blue) shows the normal expression of N-Myc. **(C)** is the higher magnification of MEF^{wt} in **(A)**. **(D-F)** MEF^{nax} staining by N-Myc (red) and DAPI (blue) display a remarkable reduction in N-Myc expression. **(F)** shows higher magnification of MEF^{nax}. **(G, H)** Western blot

analysis of N-Myc expression in MEF^{wt} and MEF^{nax} shows N-Myc protein is only 50% of MEF^{wt} in MEF^{nax} (wt: n=3 and *nax*: n=3). The actin shows the consistent loading in all MEFs samples. Scale bar = 10 μm in **(A-F)**. The data in the bar graph are presented as the mean of three independent experiments ± SEM, and statistical analysis was performed using unpaired t-test (P**<0.01).

Aim #3: To analyze whether the ubiquitin proteasome system plays a role in degradation of SHH signaling molecules in the *nax* mutant cerebellum

3.7 *The expression of 20S proteasome is slightly higher in nax mutant mouse cere bellum*

N-Myc is degraded via the ubiquitin-proteasome system and during this process, Huwe1 is a ubiquitin ligase that regulates degradation of N-Myc and balances the proliferation and differentiation of granule cell precursors (Vriend, Ghavami and Marzban; Zhao, Heng, et al.). 20S proteasome expresses in *nax* cerebellar granule cell precursors and granule cells that is comparable with wt siblings (Fig. 15, A-B). During P10 to P19, the expression of the 20S proteasome is higher in *nax* mutant while compared with wt siblings (Fig. 15, C-D).

Figure 15. The expression of 20S proteasome is slightly higher in *nax* mutant mouse

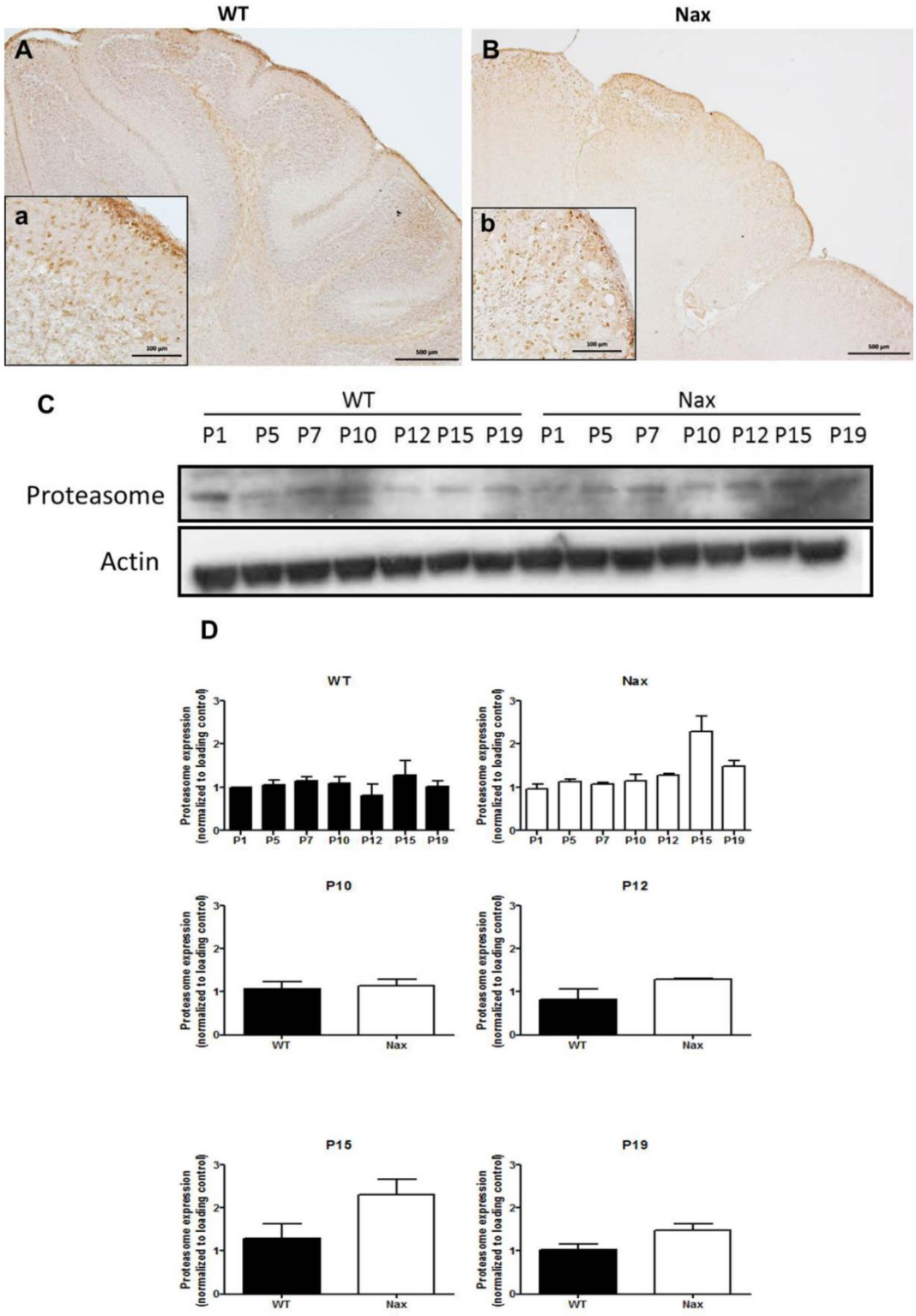

(A, B) Sagittal section of P12 wt and *nax* mutant mouse cerebellum immunostained with 20S proteasome shows the similar expression pattern. **(a)** is the higher magnification of wt cerebellum **(A)** and **(b)** shows higher magnification of *nax* cerebellum **(B)**. **(C)** Western Blot analysis of 20S proteasome expression in wt and *nax* mutant mouse cerebellum at P1, P5, P7, P10, P12, P15 and P19 reveals an overall higher expression in *nax* mutant (wt: n=3 and *nax*: n=3). The actin shows the consistent loading in all cerebellar samples. (D) Western Blot analysis of 20S proteasome expression comparison for different postnatal days between wt and *nax* mutant mouse and shows an increase from P12 and P19. The data in the bar graph are presented as the mean of three independent experiments ± SEM, and statistical analysis was performed using one-way ANOVA.

3.7.1 *The activity of 26S proteasome is higher in MEF^{nax} compared with MEF^{wt}*

20S proteasome expression increases in MEF^{nax} (Fig. 16, A-F). In order to measure accurately the 26S proteasome activity, we measured the ubiquitination activity of 20S proteasome and deubiquitination activity of 19S proteasome separately. The MEF^{nax} show much higher 20s and 19s proteasome activity when compared with MEF^{wt} (Fig. 16, G, H).

Figure 16. The activity of 26S proteasome is higher in MEF^{nax} in comparison to MEF^{wt}

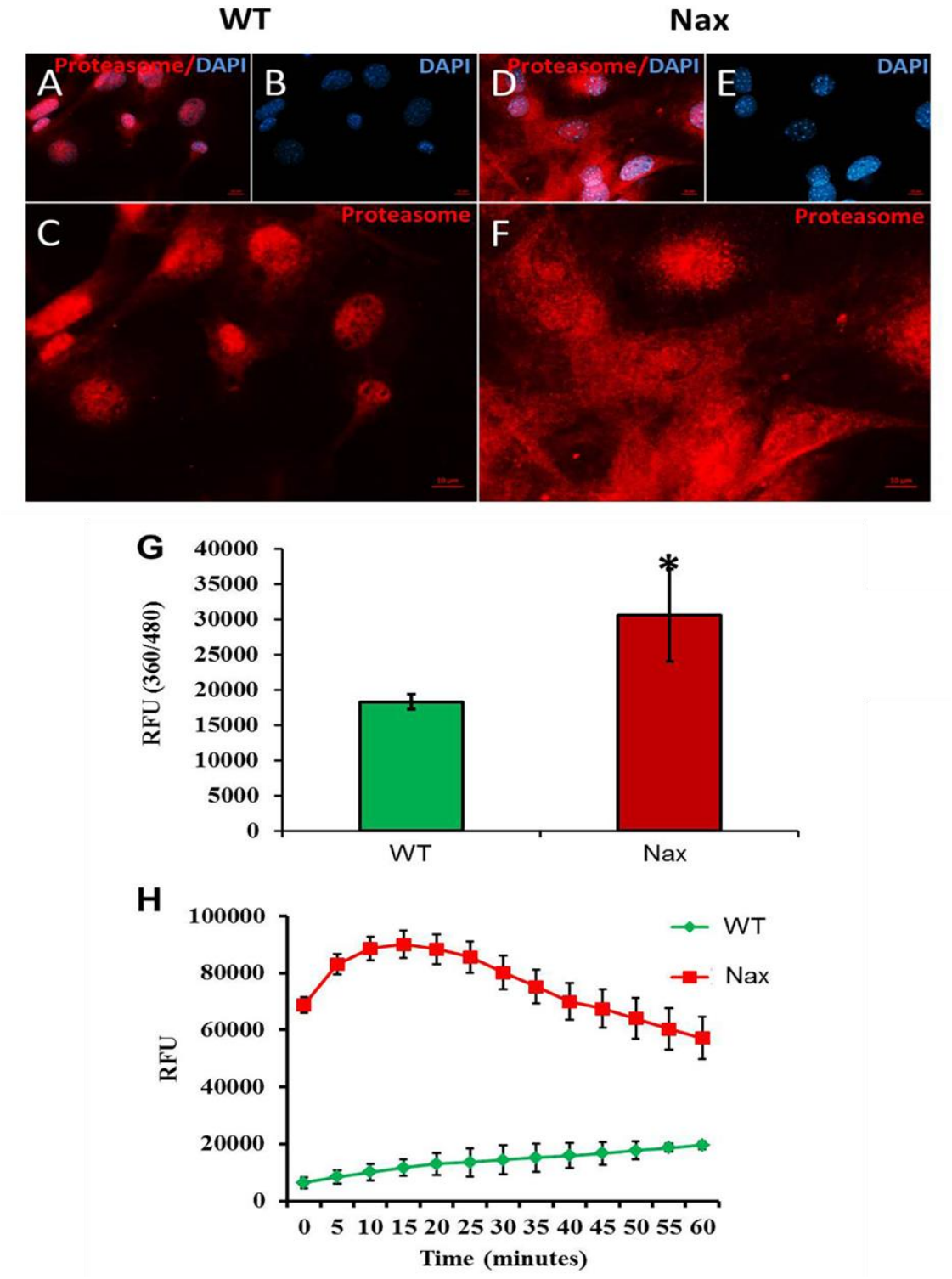

(A-C) MEF^{wt} are performed with immunofluorescence staining by 20S proteasome (red) and DAPI (blue) and show the regular expression of 20S proteasome. **(C)** is the higher magnification of MEF^{wt}. **(D-F)** MEF^{nax} are stained with proteasome (red) and DAPI (blue) and display a remarkable increase in 20S proteasome expression. **(F**) shows higher magnification of MEF^{nax}. **(G)** Measurement of 20S proteasome activity in intact 26S proteasome in MEF^{wt} and MEF^{nax}. **(H)** Measurement of 19S proteasome activity in intact 26S proteasome in MEF^{wt} and MEF^{nax}. Scale bar = 10 μm in **(A-F)**. The data in the bar graph are presented as the mean of three independent experiments ± SEM, and statistical analysis was performed using unpaired t-test.

CHAPTER 4: DISCUSSION

In *nax* mutant mouse cerebellum, the granule cells are significantly decreased that is around 20% in both vermis and hemispheres compared with wt sibling cerebellum. This severe decrease of granule cells can be deliberated due to three possibilities; 1) degeneration; 2) impairment in proliferation; 3) interruption in migration. Our lab previous work showed that the despite abundant neuronal degeneration in *nax* cerebellum, it is not suggesting the cause of cerebellar granule cell reduction when it is compared with wt sibling (Bailey, Rahimi Balaei, Mannan, et al.). In addition, in *nax* mutant cerebellum the expression pattern of Pax6 which functioned as a regulator of proliferation and differentiation showed that the granule cell proliferation is mostly impaired rather than degeneration. The Pax6 immunostaining showed the lack or thinner layer of granule cell precursors in the EGZ in *nax* cerebellum. In *nax* mutant mouse, we found that Bergmann glial cell fibers are disorganized. Despite the Bergmann glia fiber position and morphology changes in the *nax* cerebellar cortex, the small number of differentiated granule cells migrate from EGZ to granule cell layer. Thus, it is suggesting that the reduced number of the granule cells in *nax* cerebellar granule layer is due to the decreased proliferative activity of granule cell precursors during development. SHH is the primary mitogen that regulates the proliferation of granule cell precursors in the EGZ. In this study, we examined the SHH signaling pathway and its downstream molecules in *nax* mutant mouse cerebellum to understand whether the reduced granule cell precursors and granule cells are associated with impaired SHH signaling pathway. SHH expression

shows a similar trend in wt and *nax* mutant mouse cerebellum. However, the overall SHH expression is lower in *nax* mutant cerebellum and reaches the peak at P7, while in wt sibling, the peak is at around P10. The readout of activated SHH signaling pathway factor Gli1 expresses and distributes in the granule cell precursors and Purkinje cells in the *nax* cerebellar cortex which is comparable with wt sibling cerebellar cortex. Interestingly, the N-Myc expression level in *nax* cerebellum is lower when it is compared with the wt sibling cerebellum. The lower expression of N-Myc is shown in *nax* mutant MEF cells (MEF^{nax}) by immunocytochemistry and Western blot analysis. In addition, the down-regulated N-Myc is accompanied by a high expression level of 20S proteasome and high activity of 26S proteasome function in MEF^{nax}. Thus, our findings suggest that the granule cell precursors proliferation impairment in *nax* cerebellum is associated with the down-regulation of N-Myc which is accomplished by ubiquitin proteasome system overactivity.

4.1 Dysregulation of the SHH signaling pathway in *nax* mutant mouse

Numerous studies have indicated that SHH pathway plays a crucial role in granule cell precursors proliferation in the cerebellum (Corrales, Rocco, et al.; Haldipur et al.; Lewis et al.; Wechsler-Reya and Scott). It has been shown that the proliferative activity of the granule cell precursors significantly reduced after treatment of the P12 mouse with neutralizing SHH by the anti-SHH monoclonal antibody (Wallace). The reduced proliferative activity of the granule cell precursors has been shown both *in vitro* and *in*

vivo experiments (Wallace). Several important mitogens have been identified and studied, such as SHH, epidermal growth factor and plasminogen activator in the cerebellum (Kitchens, Snyder and Gottlieb; Moonen et al.). Among those, SHH was considered as the most effective mitogenic factor because it promotes proliferative activity at around 100 times more than other factors on the granule cell precursors in EGZ (Wechsler-Reya and Scott). It is also reported that SHH stimulates the PTCH1 and Gli1 transcription factor and form a feedback loop in which increases the proliferative activity. In addition, this mitogenic effect was limited during the postnatal development based on the study of SMO-deleted conditional knock-out mouse (Corrales, Blaess, et al.).

Medulloblastoma is one of the most common malignant brain tumors which is classified into four types: WNT/β-catenin, Sonic Hedgehog, Group 3, and Group 4 (Roussel and Hatten; Taylor et al.). SHH and its downstream pathway molecules (PTCH1, SMO, SUFU etc.) malfunction are associated with over-proliferation of granule cell precursor and form the SHH type of the medulloblastoma (Marino; Gibson et al.). Many studies have suggested that inhibition of the SHH pathway may be a novel therapeutic approach for SHH medulloblastoma. HhAntag which is a small molecule inhibited SMO in SHH signaling pathway and suppressed the granule cell proliferation and with a high dose, eradicated the tumor and increased the animal lifespan (Romer et al.). Lee et al., (2012) showed another SHH pathway inhibitor which called saridegib (IPI-926) prolonged the survival of the mouse model for medulloblastoma (M. J. Lee et al.). These studies strongly indicate the pivotal role of SHH pathway in regulating granule cell

development and proliferation.

SHH is a morphogen that plays an important role in cell fate which depends on the exposure time and concentration (Roelink et al.). Higher concentration of the SHH is found in the ventral regions of the neural tube while the lower concentration at dorsal part (Ribes and Briscoe). The slight changes of the SHH expression pattern may result in a massive difference in cell fate which cannot be excluded in the *nax* mutant cerebellar cortex cell fate.

The most proliferative granule cell precursors are located in the outer layer of EGZ and display a high level of Gli1 expression (Dahmane and Ruiz i Altaba). Gli1 is belonged to the Gli family and participate in many cellular activities, such as cell fate determination, cell patterning and cell proliferation (Corrales, Rocco, et al.; Ma et al.). Examination of Gli1 – the activator of SHH pathway (Haldipur et al.) in *nax* mutant suggested that the synthesis and expression of SHH and Gli1 proteins are comparable in *nax* mutant and wt sibling cerebellum.

4.2 N-Myc expression is downregulated in *nax* mutant mouse

Myc family are associated with cell proliferation within different tissues in the body. N-Myc as one of the Gli target gene in SHH pathway is also important for granule cell precursors proliferation (Mill et al.; Oliver et al.; Kenney, Cole and Rowitch; Knoepfler, Cheng and Eisenman). The *MYCN* gene is found amplified repeatedly in metastatic human neuroblastomas and serves as a transcription factor that participates in many

cellular processes containing proliferation, differentiation and apoptosis (Grandori et al.). Sawai et al., (1991), Charron et al., (1992) and Stanton et al., (1992) demonstrated that the disruption of N-Myc expression results in embryonic lethality at mid-gestation by studying N-Myc knockout mouse (Charron et al.; Sawai et al.; Stanton et al.). Nagy et al., (1998) were able to delay and reduce lethality rate of the heterozygous $N\text{-}Myc^{Lneo}/N\text{-}Myc^{Plox}$ by controlling N-Myc expression level (Nagy et al.). With the conditionally targeted N-Myc mice, Knoepfler et al., (2002) focused on the nervous system development and found that impaired N-Myc expression disturbs the neuronal progenitor proliferation and differentiation. The conditional N-Myc knockout mouse showed ataxia, growth retardation accompany with a two folds reduction in brain mass (Knoepfler, Cheng and Eisenman). They also showed that there is a severe impairment in cerebellar development including small size, disorganized and damaged foliation. The granule layer was thin and the density at around 10%-30% when it was compared with control mouse. It has also been shown that in conditional deletion of N-Myc mouse, the SHH pathway was interrupted with an 8-fold reduction of granule cell precursors compare with the control group (Hatton et al.).

Besides depleting N-Myc expression, Hatton et al., (2006) generated the ND2:SmoA1 mice which displayed an increased population of granule cells and a hyperproliferation of granule cell precursors in EGZ (Hatton et al.). At P20, there were still some Ki-67 and Nestin positive cells in EGZ which indicate granule cell development persisted at progenitor functional level. In this mouse, the expression of

N-Myc was increased in the cerebellum which was shown by real-time PCR analysis. At 6 months old, around 33% mice formed the medulloblastoma. They generated a combined N-Myc conditional knockout × ND2:SmoA1 mice. This mouse was similar to the N-Myc conditional knockout mouse with underdeveloped cerebellar foliation and a reduced granule cell layer regardless of *SMO* gene expression (Hatton et al.). Furthermore, Oliver et al., (2003) proved that N-Myc is an important factor for cell proliferation when it was treated with SHH using granule cell precursors culture (Oliver et al.).

The reduction of granule cells in these studies are similar to our *nax* mutant mouse that indicate the N-Myc is probably the potential pivotal factor which is associated to granule cell precursors proliferative impairment in the *nax* cerebellum during development. Unlike SHH, we have shown that the N-Myc has a striking alteration in *nax* mutant mouse cerebellum. Therefore, it is indicating that N-Myc is required for SHH signaling pathway and plays an important role in expanding the granule cell precursors in EGZ during cerebellum development. The detailed molecular mechanism and N-Myc downregulation in *nax* mutant were explored using *nax* and wt MEF cells. It is revealed that in MEF^{nax} the N-Myc expression is significantly reduced by using immunostaining and Western blot analysis in comparison to the MEF^{wt}. The lower expression of N-Myc is either due to the lower synthesis of N-Myc protein or higher elimination activities after protein synthesis. Therefore, we further investigated the proteasome system which plays an essential role in regulating N-Myc function (Vriend, Ghavami and Marzban; Zhao, D,

et al.; Zhao, Heng, et al.). According to the slight alteration in the expression of SHH and Gli1, we are inclined to the latter possibility.

4.3 20S Proteasome expression and activity is higher in *nax* mutant mouse

The ubiquitin-proteasome system is a complex of the component cells that retains the proteostasis and responsible for rapidly and efficiently breaking down the unwanted or misfolded proteins. Switching from the cell cycle processes to differentiation at the accurate and particular time point by degradation of some mitogens is a very important phase that ensure the formation of the correct population of neurons during neurogenesis and corticogenesis (Kintner). Due to the degradation function of the ubiquitin-proteasome system, N-Myc is known as a short-lived protein with a half-life of 30min (Cohn et al.).

In the ubiquitin-proteasome system, ligase such as Huwe1 and other ligases are responsible for breaking down N-Myc protein (Zhao, Heng, et al.; King et al.; Zhao, D, et al.). Zhao et al., (2008) has shown that the endogenous N-Myc binds to Huwe1 and degraded by the proteasome (Zhao, Heng, et al.). The ubiquitin-mediated degradation of the N-Myc protein withdraws the cells from proliferation and initiates the differentiation. This was supported by Huwe1 knockout cells, in which the N-Myc level was maintained which resulted in impairment of the ES cell differentiation. After silencing of N-Myc, the Huwe1 knockout cells restored neural differentiation which proved that Huwe1 withdraws the cell cycle process and encourages the differentiation via degradation of N-Myc protein (Zhao, Heng, et al.). Zhao et al., (2009) also generated a conditional

Huwe1 knockout mouse to explore the N-Myc degradation by ubiquitin proteasome system (Zhao, D, et al.). In their study, this conditional knockout mouse displayed the prolonged cell cycle process and causes dysregulation in cell differentiation (Zhao, D, et al.).

In our study, the activity of ubiquitin proteasome system was examined to determine if the alteration of ubiquitin proteasome system is responsible for the decreased N-Myc protein and ultimately stops the proliferation of granule cell precursors. We used MEFs to establish this experiment and discovered that the activity of ubiquitin proteasome system in MEF^{nax} is strikingly increased which means the clearance process of many proteins are accelerated. Therefore it is suggesting that N-Myc degradation is involved in these processes. It may suggest that the expression level of ligase such as Huwe1 increased in *nax* mutant. Finally, this study suggests that the altered ubiquitin proteasome system and probably Huwe1 are critical for N-Myc degradation and may be underneath the molecular mechanism of the granule cells reduction in *nax* mutant mouse cerebellum.

CHAPTER 5: CONCLUSION AND FUTURE DIRECTION

SHH signaling is a well-studied pathway that participates in many developmental processes including growth, cell proliferation, differentiation and patterning of the central nervous system. Numerous studies have demonstrated that the SHH function is prominent and manifests differently at different concentration and time point. N-Myc as a downstream molecule of SHH signaling pathway has been shown to promote the proliferation of granule cell precursors in cerebellum. In this study, the several important factors in SHH signaling pathway have been studied in *nax* mutant mouse cerebellum to investigate the possible mechanism underneath the cerebellar granule cell reduction. In wt sibling mouse, the granule layer is composed of packed numerous granule cells which comprise about 80% of the neurons in the brain. However, in *nax* mutant mouse cerebellum, the number of granule cells and the granule cell precursors are only around 20% of the wt sibling. We showed that the SHH signaling pathway is activated in both wt sibling and *nax* mutant mouse cerebellum however with a decrease in *nax* mutant cerebellum. In addition, we demonstrated that N-Myc has a striking alteration in *nax* mutant mouse along with the elevated activity of proteasome in MEF^{nax}. Together, these findings suggest an essential role of N-Myc in granule cell precursors proliferation and showed that the regulation of N-Myc accomplished by ubiquitin proteasome system which is probably damaged in *nax* cerebellum and serve as a potential mechanism underneath the reduced granule cells in *nax* mutant cerebellum.

For future direction of this study, some more experiments need to be done to address

some important questions. First, it needs to investigate the ubiquitin ligases that are responsible for the degradation of other molecules in the SHH signaling pathway, for example, SHH and N-Myc. The Huwe1 ligase needs to be investigated which is important to solid the theory that degradation of N-Myc depends on the proteasome. Second, it is better to confirm the results of the MEFs with cerebellar granule cell precursors culture which is more reliable due to MEFs are the fibroblasts origin instead of neurons. The experiments with cerebellar granule cell precursors culture can demonstrate the N-Myc expression level and its regulation by ligase such as Huwe1. The last but not least, we can generate the conditional Huwe1 knockout × Acp2 mutant mouse to further confirm the function of Huwe1 and may rescue the *nax* mutant mouse.

REFERENCE

Aguilar, A., et al. "Analysis of Human Samples Reveals Impaired Shh-Dependent Cerebellar Development in Joubert Syndrome/Meckel Syndrome." *Proc Natl Acad Sci U S A* 109.42 (2012): 16951-6. Print.

Ashtari, N, et al. "Lysosomal Acid Phosphatase Biosynthesis and Dysfunction: A Mini Review Focused on Lysosomal Enzyme Dysfunction in Brain." *Current molecular medicine* 16.5 (2016): 439-46. Print.

Azevedo, F. A., et al. "Equal Numbers of Neuronal and Nonneuronal Cells Make the Human Brain an Isometrically Scaled-up Primate Brain." *J Comp Neurol* 513.5 (2009): 532-41. Print.

Bailey, K., et al. "Purkinje Cell Compartmentation in the Cerebellum of the Lysosomal Acid Phosphatase 2 Mutant Mouse (Nax - Naked-Ataxia Mutant Mouse)." *PLoS One* 9.4 (2014): e94327. Print.

Bailey, K., et al. "Spatial and Temporal Expression of Lysosomal Acid Phosphatase 2 (Acp2) Reveals Dynamic Patterning of the Mouse Cerebellar Cortex." *Cerebellum* 12.6 (2013): 870-81. Print.

Bogaert, M. G., and F. M. Belpaire. "[Studies of Papaverine Metabolism in Animals]." *Verh K Acad Geneeskd Belg* 39.2 (1977): 65-103. Print.

Brickley, S. G., S. G. Cull-Candy, and M. Farrant. "Development of a Tonic Form of Synaptic Inhibition in Rat Cerebellar Granule Cells Resulting from Persistent Activation of Gabaa Receptors." *J Physiol* 497 (Pt 3) (1996): 753-9. Print.

Bumcrot, D. A., R. Takada, and A. P. McMahon. "Proteolytic Processing Yields Two Secreted Forms of Sonic Hedgehog." *Mol Cell Biol* 15.4 (1995): 2294-303. Print.

Butts, T., M. J. Green, and R. J. Wingate. "Development of the Cerebellum: Simple Steps to Make a 'Little Brain'." *Development* 141.21 (2014): 4031-41. Print.

Charron, J., et al. "Embryonic Lethality in Mice Homozygous for a Targeted Disruption of the N-Myc Gene." *Genes Dev* 6.12A (1992): 2248-57. Print.

Chaumont, Joseph, et al. "Clusters of Cerebellar Purkinje Cells Control Their Afferent Climbing Fiber Discharge." *Proceedings of the National Academy of Sciences* 110.40 (2013): 16223-28. Print.

Cohn, S. L., et al. "Prolonged N-Myc Protein Half-Life in a Neuroblastoma Cell Line Lacking N-Myc Amplification." *Oncogene* 5.12 (1990): 1821-7. Print.

Corcoran, R. B., and M. P. Scott. "Oxysterols Stimulate Sonic Hedgehog Signal Transduction and Proliferation of Medulloblastoma Cells." *Proc Natl Acad Sci U S A* 103.22 (2006): 8408-13. Print.

Corrales, J. D., et al. "The Level of Sonic Hedgehog Signaling Regulates the Complexity of Cerebellar Foliation." *Development* 133.9 (2006): 1811-21. Print.

Corrales, J. D., et al. "Spatial Pattern of Sonic Hedgehog Signaling through Gli Genes During Cerebellum Development." *Development* 131.22 (2004): 5581-90. Print.

D'Arca, D., et al. "Huwe1 Ubiquitin Ligase Is Essential to Synchronize Neuronal and

Glial Differentiation in the Developing Cerebellum." *Proc Natl Acad Sci U S A* 107.13 (2010): 5875-80. Print.

da Costa, N. M., and K. A. Martin. "How Thalamus Connects to Spiny Stellate Cells in the Cat's Visual Cortex." *J Neurosci* 31.8 (2011): 2925-37. Print.

Dahmane, N., and A. Ruiz i Altaba. "Sonic Hedgehog Regulates the Growth and Patterning of the Cerebellum." *Development* 126.14 (1999): 3089-100. Print.

Dino, MR, et al. "Unipolar Brush Cell: A Potential Feedforward Excitatory Interneuron of the Cerebellum." *Neuroscience* 98.4 (2000): 625-36. Print.

Doya, K. "Complementary Roles of Basal Ganglia and Cerebellum in Learning and Motor Control." *Curr Opin Neurobiol* 10.6 (2000): 732-9. Print.

Duester, G. "Retinoic Acid Synthesis and Signaling During Early Organogenesis." *Cell* 134.6 (2008): 921-31. Print.

Eccles, J., R. Llinas, and K. Sasaki. "Golgi Cell Inhibition in the Cerebellar Cortex." *Nature* 204 (1964): 1265-6. Print.

Echelard, Yann, et al. "Sonic Hedgehog, a Member of a Family of Putative Signaling Molecules, Is Implicated in the Regulation of Cns Polarity." *Cell* 75.7 (1993): 1417-30. Print.

Fine, E. J., C. C. Ionita, and L. Lohr. "The History of the Development of the Cerebellar Examination." *Semin Neurol* 22.4 (2002): 375-84. Print.

Fink, A. J., et al. "Development of the Deep Cerebellar Nuclei: Transcription Factors and Cell Migration from the Rhombic Lip." *J Neurosci* 26.11 (2006): 3066-76. Print.

Freund, T. F., I. Katona, and D. Piomelli. "Role of Endogenous Cannabinoids in Synaptic Signaling." *Physiol Rev* 83.3 (2003): 1017-66. Print.

Ganguly, K., et al. "Gaba Itself Promotes the Developmental Switch of Neuronal Gabaergic Responses from Excitation to Inhibition." *Cell* 105.4 (2001): 521-32. Print.

Gibson, P., et al. "Subtypes of Medulloblastoma Have Distinct Developmental Origins." *Nature* 468.7327 (2010): 1095-9. Print.

Grandori, C., et al. "The Myc/Max/Mad Network and the Transcriptional Control of Cell Behavior." *Annu Rev Cell Dev Biol* 16 (2000): 653-99. Print.

Gray, Jason, and M Elizabeth Ross. "Neural Tube Closure in Mouse Whole Embryo Culture." *Journal of visualized experiments: JoVE*.56 (2011). Print.

Haas, A. L., et al. "Ubiquitin-Activating Enzyme. Mechanism and Role in Protein-Ubiquitin Conjugation." *J Biol Chem* 257.5 (1982): 2543-8. Print.

Haldipur, P., et al. "Expression of Sonic Hedgehog During Cell Proliferation in the Human Cerebellum." *Stem Cells Dev* 21.7 (2012): 1059-68. Print.

Hatton, B. A., et al. "N-Myc Is an Essential Downstream Effector of Shh Signaling During Both Normal and Neoplastic Cerebellar Growth." *Cancer Res* 66.17 (2006): 8655-61. Print.

Heikinheimo, M., et al. "Fgf-8 Expression in the Post-Gastrulation Mouse Suggests Roles in the Development of the Face, Limbs and Central Nervous System." *Mech Dev*

48.2 (1994): 129-38. Print.
Hevner, R. F. "From Radial Glia to Pyramidal-Projection Neuron: Transcription Factor Cascades in Cerebral Cortex Development." *Mol Neurobiol* 33.1 (2006): 33-50. Print.
Ingham, P. W., Y. Nakano, and C. Seger. "Mechanisms and Functions of Hedgehog Signalling across the Metazoa." *Nat Rev Genet* 12.6 (2011): 393-406. Print.
Jacob, J., and J. Briscoe. "Gli Proteins and the Control of Spinal-Cord Patterning." *EMBO Rep* 4.8 (2003): 761-5. Print.
Jakab, R. L., and J. Hamori. "Quantitative Morphology and Synaptology of Cerebellar Glomeruli in the Rat." *Anat Embryol (Berl)* 179.1 (1988): 81-8. Print.
Johnson, R. L., et al. "Human Homolog of Patched, a Candidate Gene for the Basal Cell Nevus Syndrome." *Science* 272.5268 (1996): 1668-71. Print.
Katahira, T., et al. "Interaction between Otx2 and Gbx2 Defines the Organizing Center for the Optic Tectum." *Mech Dev* 91.1-2 (2000): 43-52. Print.
Kenney, A. M., M. D. Cole, and D. H. Rowitch. "Nmyc Upregulation by Sonic Hedgehog Signaling Promotes Proliferation in Developing Cerebellar Granule Neuron Precursors." *Development* 130.1 (2003): 15-28. Print.
Kenney, A. M., and D. H. Rowitch. "Sonic Hedgehog Promotes G(1) Cyclin Expression and Sustained Cell Cycle Progression in Mammalian Neuronal Precursors." *Mol Cell Biol* 20.23 (2000): 9055-67. Print.
King, B., et al. "The Ubiquitin Ligase Huwe1 Regulates the Maintenance and Lymphoid Commitment of Hematopoietic Stem Cells." *Nat Immunol* 17.11 (2016): 1312-21. Print.
Kintner, C. "Neurogenesis in Embryos and in Adult Neural Stem Cells." *J Neurosci* 22.3 (2002): 639-43. Print.
Kitchens, D. L., E. Y. Snyder, and D. I. Gottlieb. "Fgf and Egf Are Mitogens for Immortalized Neural Progenitors." *J Neurobiol* 25.7 (1994): 797-807. Print.
Knoepfler, P. S., P. F. Cheng, and R. N. Eisenman. "N-Myc Is Essential During Neurogenesis for the Rapid Expansion of Progenitor Cell Populations and the Inhibition of Neuronal Differentiation." *Genes Dev* 16.20 (2002): 2699-712. Print.
Kuriyama, K., and P. Y. Sze. "Blood-Brain Barrier to H3-Gamma-Aminobutyric Acid in Normal and Amino Oxyacetic Acid-Treated Animals." *Neuropharmacology* 10.1 (1971): 103-8. Print.
Lee, Kevin J, and Thomas M Jessell. "The Specification of Dorsal Cell Fates in the Vertebrate Central Nervous System." *Annual review of neuroscience* 22.1 (1999): 261-94. Print.
Lee, M. J., et al. "Hedgehog Pathway Inhibitor Saridegib (Ipi-926) Increases Lifespan in a Mouse Medulloblastoma Model." *Proc Natl Acad Sci U S A* 109.20 (2012): 7859-64. Print.
Lee, S. J., et al. "Sonic Hedgehog-Induced Histone Deacetylase Activation Is Required for Cerebellar Granule Precursor Hyperplasia in Medulloblastoma." *PLoS One* 8.8

(2013): e71455. Print.
Leto, Ketty, et al. "Consensus Paper: Cerebellar Development." *The Cerebellum* 15.6 (2016): 789-828. Print.
Lewis, P. M., et al. "Sonic Hedgehog Signaling Is Required for Expansion of Granule Neuron Precursors and Patterning of the Mouse Cerebellum." *Dev Biol* 270.2 (2004): 393-410. Print.
Litingtung, Y., and C. Chiang. "Control of Shh Activity and Signaling in the Neural Tube." *Dev Dyn* 219.2 (2000): 143-54. Print.
Llinas, Rodolfo, and Mario N Negrello. "Cerebellum." *Scholarpedia* 10.1 (2015): 4606. Print.
Lubke, T., P. Lobel, and D. E. Sleat. "Proteomics of the Lysosome." *Biochim Biophys Acta* 1793.4 (2009): 625-35. Print.
Ma, M., et al. "N-Myc Is a Key Switch Regulating the Proliferation Cycle of Postnatal Cerebellar Granule Cell Progenitors." *Sci Rep* 5 (2015): 12740. Print.
Machold, R., and G. Fishell. "Math1 Is Expressed in Temporally Discrete Pools of Cerebellar Rhombic-Lip Neural Progenitors." *Neuron* 48.1 (2005): 17-24. Print.
Makrypidi, G., et al. "Mannose 6 Dephosphorylation of Lysosomal Proteins Mediated by Acid Phosphatases Acp2 and Acp5." *Mol Cell Biol* 32.4 (2012): 774-82. Print.
Mallet, J., et al. "Anatomical, Physiological and Biochemical Studies on the Cerebellum from Mutant Mice. Iii. Protein Differences Associated with the Weaver, Staggerer and Nervous Mutations." *Brain Res* 103.2 (1976): 291-312. Print.
Mannan, A. U., et al. "Mutation in the Gene Encoding Lysosomal Acid Phosphatase (Acp2) Causes Cerebellum and Skin Malformation in Mouse." *Neurogenetics* 5.4 (2004): 229-38. Print.
Marigo, V., et al. "Cloning, Expression, and Chromosomal Location of Shh and Ihh: Two Human Homologues of the Drosophila Segment Polarity Gene Hedgehog." *Genomics* 28.1 (1995): 44-51. Print.
Marino, S. "Medulloblastoma: Developmental Mechanisms out of Control." *Trends Mol Med* 11.1 (2005): 17-22. Print.
Marr, D. "A Theory of Cerebellar Cortex." *J Physiol* 202.2 (1969): 437-70. Print.
Martinez-Ferre, Almudena, and Salvador Martinez. "Molecular Regionalization of the Diencephalon." *Frontiers in neuroscience* 6 (2012). Print.
Marzban, H., et al. "Cellular Commitment in the Developing Cerebellum." *Front Cell Neurosci* 8 (2014): 450. Print.
Merchant, M., et al. "Suppressor of Fused Regulates Gli Activity through a Dual Binding Mechanism." *Mol Cell Biol* 24.19 (2004): 8627-41. Print.
Mill, P., et al. "Shh Controls Epithelial Proliferation Via Independent Pathways That Converge on N-Myc." *Dev Cell* 9.2 (2005): 293-303. Print.
Mimeault, M., and S. K. Batra. "Frequent Deregulations in the Hedgehog Signaling Network and Cross-Talks with the Epidermal Growth Factor Receptor Pathway Involved in Cancer Progression and Targeted Therapies." *Pharmacol Rev* 62.3

(2010): 497-524. Print.
Mishina, Masayoshi, et al. "Molecular Mechanism of Parallel Fiber-Purkinje Cell Synapse Formation." *Frontiers in neural circuits* 6 (2012). Print.
Moonen, G., et al. "Plasminogen Activator Is a Mitogen for Astrocytes in Developing Cerebellum." *Brain Res* 352.1 (1985): 41-8. Print.
Mugnaini, Enrico, Gabriella Sekerková, and Marco Martina. "The Unipolar Brush Cell: A Remarkable Neuron Finally Receiving Deserved Attention." *Brain research reviews* 66.1 (2011): 220-45. Print.
Muller, F., and R. O'Rahilly. "The Human Brain at Stage 16, Including the Initial Evagination of the Neurohypophysis." *Anat Embryol (Berl)* 179.6 (1989): 551-69. Print.
---. "The Human Brain at Stages 18-20, Including the Choroid Plexuses and the Amygdaloid and Septal Nuclei." *Anat Embryol (Berl)* 182.3 (1990): 285-306. Print.
---. "The Human Brain at Stages 21-23, with Particular Reference to the Cerebral Cortical Plate and to the Development of the Cerebellum." *Anat Embryol (Berl)* 182.4 (1990): 375-400. Print.
Nagy, A., et al. "Dissecting the Role of N-Myc in Development Using a Single Targeting Vector to Generate a Series of Alleles." *Curr Biol* 8.11 (1998): 661-4. Print.
Nakamura, Harukazu, et al. "Isthmus Organizer for Midbrain and Hindbrain Development." *Brain research reviews* 49.2 (2005): 120-26. Print.
Nassif, N. D., S. E. Cambray, and D. A. Kraut. "Slipping Up: Partial Substrate Degradation by Atp-Dependent Proteases." *IUBMB Life* 66.5 (2014): 309-17. Print.
Nusslein-Volhard, C., and E. Wieschaus. "Mutations Affecting Segment Number and Polarity in Drosophila." *Nature* 287.5785 (1980): 795-801. Print.
Obrietan, K., X. B. Gao, and A. N. Van Den Pol. "Excitatory Actions of Gaba Increase Bdnf Expression Via a Mapk-Creb-Dependent Mechanism--a Positive Feedback Circuit in Developing Neurons." *J Neurophysiol* 88.2 (2002): 1005-15. Print.
Oliver, T. G., et al. "Transcriptional Profiling of the Sonic Hedgehog Response: A Critical Role for N-Myc in Proliferation of Neuronal Precursors." *Proc Natl Acad Sci U S A* 100.12 (2003): 7331-6. Print.
Pepinsky, R. B., et al. "Identification of a Palmitic Acid-Modified Form of Human Sonic Hedgehog." *J Biol Chem* 273.22 (1998): 14037-45. Print.
Petroff, O. A. "Gaba and Glutamate in the Human Brain." *Neuroscientist* 8.6 (2002): 562-73. Print.
Platt, F. M., B. Boland, and A. C. van der Spoel. "The Cell Biology of Disease: Lysosomal Storage Disorders: The Cellular Impact of Lysosomal Dysfunction." *J Cell Biol* 199.5 (2012): 723-34. Print.
Pohlmann, R., et al. "Human Lysosomal Acid Phosphatase: Cloning, Expression and Chromosomal Assignment." *EMBO J* 7.8 (1988): 2343-50. Print.

Rakic, P. "Evolution of the Neocortex: A Perspective from Developmental Biology." *Nat Rev Neurosci* 10.10 (2009): 724-35. Print.

Ribes, V., and J. Briscoe. "Establishing and Interpreting Graded Sonic Hedgehog Signaling During Vertebrate Neural Tube Patterning: The Role of Negative Feedback." *Cold Spring Harb Perspect Biol* 1.2 (2009): a002014. Print.

Roelink, H., et al. "Floor Plate and Motor Neuron Induction by Different Concentrations of the Amino-Terminal Cleavage Product of Sonic Hedgehog Autoproteolysis." *Cell* 81.3 (1995): 445-55. Print.

Romer, J. T., et al. "Suppression of the Shh Pathway Using a Small Molecule Inhibitor Eliminates Medulloblastoma in Ptc1(+/-)P53(-/-) Mice." *Cancer Cell* 6.3 (2004): 229-40. Print.

Roussel, M. F., and M. E. Hatten. "Cerebellum Development and Medulloblastoma." *Curr Top Dev Biol* 94 (2011): 235-82. Print.

Ruiz-Gomez, A., et al. "The Cell Biology of Smo Signalling and Its Relationships with Gpcrs." *Biochim Biophys Acta* 1768.4 (2007): 901-12. Print.

Ruiz i Altaba, A. "Gli Proteins and Hedgehog Signaling: Development and Cancer." *Trends Genet* 15.10 (1999): 418-25. Print.

---. "Gli Proteins Encode Context-Dependent Positive and Negative Functions: Implications for Development and Disease." *Development* 126.14 (1999): 3205-16. Print.

Ruppert, J. M., et al. "The Gli-Kruppel Family of Human Genes." *Mol Cell Biol* 8.8 (1988): 3104-13. Print.

Saftig, P., and J. Klumperman. "Lysosome Biogenesis and Lysosomal Membrane Proteins: Trafficking Meets Function." *Nat Rev Mol Cell Biol* 10.9 (2009): 623-35. Print.

Sawai, S., et al. "Embryonic Lethality Resulting from Disruption of Both N-Myc Alleles in Mouse Zygotes." *New Biol* 3.9 (1991): 861-9. Print.

Schulman, J. M., et al. "Multiple Hereditary Infundibulocystic Basal Cell Carcinoma Syndrome Associated with a Germline Sufu Mutation." *JAMA Dermatol* 152.3 (2016): 323-7. Print.

Schwab, M., et al. "Amplified DNA with Limited Homology to Myc Cellular Oncogene Is Shared by Human Neuroblastoma Cell Lines and a Neuroblastoma Tumour." *Nature* 305.5931 (1983): 245-8. Print.

Shows, T. B., J. A. Brown, and P. A. Lalley. "Assignment and Linear Order of Human Acid Phosphatase-2, Esterase A4, and Lactate Dehydrogenase a Genes on Chromosome 11." *Cytogenet Cell Genet* 16.1-5 (1976): 231-4. Print.

Smith, Jodi L, and Gary C Schoenwolf. "Neurulation: Coming to Closure." *Trends in neurosciences* 20.11 (1997): 510-17. Print.

Stanton, B. R., et al. "Loss of N-Myc Function Results in Embryonic Lethality and Failure of the Epithelial Component of the Embryo to Develop." *Genes Dev* 6.12A (1992): 2235-47. Print.

Steinlin, M. "Cerebellar Disorders in Childhood: Cognitive Problems." *Cerebellum* 7.4

(2008): 607-10. Print.
Strutt, H., et al. "Mutations in the Sterol-Sensing Domain of Patched Suggest a Role for Vesicular Trafficking in Smoothened Regulation." *Curr Biol* 11.8 (2001): 608-13. Print.
Taipale, J., et al. "Patched Acts Catalytically to Suppress the Activity of Smoothened." *Nature* 418.6900 (2002): 892-7. Print.
Taylor, M. D., et al. "Molecular Subgroups of Medulloblastoma: The Current Consensus." *Acta Neuropathol* 123.4 (2012): 465-72. Print.
Teng, Ching Sung, et al. "Neuroembryology and Neurogenesis." *Neuroscience in Medicine*. Springer, 2003. 111-28. Print.
Thach, W. T. "On the Mechanism of Cerebellar Contributions to Cognition." *Cerebellum* 6.3 (2007): 163-7. Print.
Tia, S., et al. "Developmental Changes of Inhibitory Synaptic Currents in Cerebellar Granule Neurons: Role of Gaba(a) Receptor Alpha 6 Subunit." *J Neurosci* 16.11 (1996): 3630-40. Print.
Tsekhmistrenko, T. A. "Quantitative Changes in Human Cerebellar Pyriform Neurons from Birth to the Age of 20 Years." *Neurosci Behav Physiol* 29.4 (1999): 405-9. Print.
Tyrrell, T., and D. Willshaw. "Cerebellar Cortex: Its Simulation and the Relevance of Marr's Theory." *Philos Trans R Soc Lond B Biol Sci* 336.1277 (1992): 239-57. Print.
Vriend, J., S. Ghavami, and H. Marzban. "The Role of the Ubiquitin Proteasome System in Cerebellar Development and Medulloblastoma." *Mol Brain* 8.1 (2015): 64. Print.
Wadiche, J. I., and C. E. Jahr. "Multivesicular Release at Climbing Fiber-Purkinje Cell Synapses." *Neuron* 32.2 (2001): 301-13. Print.
Wallace, V. A. "Purkinje-Cell-Derived Sonic Hedgehog Regulates Granule Neuron Precursor Cell Proliferation in the Developing Mouse Cerebellum." *Curr Biol* 9.8 (1999): 445-8. Print.
Wassarman, K. M., et al. "Specification of the Anterior Hindbrain and Establishment of a Normal Mid/Hindbrain Organizer Is Dependent on Gbx2 Gene Function." *Development* 124.15 (1997): 2923-34. Print.
Watanabe, M., et al. "Gaba and Gaba Receptors in the Central Nervous System and Other Organs." *Int Rev Cytol* 213 (2002): 1-47. Print.
Wechsler-Reya, R. J., and M. P. Scott. "Control of Neuronal Precursor Proliferation in the Cerebellum by Sonic Hedgehog." *Neuron* 22.1 (1999): 103-14. Print.
Wingate, R. J. "The Rhombic Lip and Early Cerebellar Development." *Curr Opin Neurobiol* 11.1 (2001): 82-8. Print.
Wolf, U., M. J. Rapoport, and T. A. Schweizer. "Evaluating the Affective Component of the Cerebellar Cognitive Affective Syndrome." *J Neuropsychiatry Clin Neurosci* 21.3 (2009): 245-53. Print.

Wurst, Wolfgang, and Laure Bally-Cuif. "Neural Plate Patterning: Upstream and Downstream of the Isthmic Organizer." *Nature Reviews Neuroscience* 2.2 (2001): 99-108. Print.

Xu, H., and D. Ren. "Lysosomal Physiology." *Annu Rev Physiol* 77 (2015): 57-80. Print.

Yacubova, E., and H. Komuro. "Cellular and Molecular Mechanisms of Cerebellar Granule Cell Migration." *Cell Biochem Biophys* 37.3 (2003): 213-34. Print.

Yamada, K., and M. Watanabe. "Cytodifferentiation of Bergmann Glia and Its Relationship with Purkinje Cells." *Anat Sci Int* 77.2 (2002): 94-108. Print.

Yeung, J., et al. "Wls Provides a New Compartmental View of the Rhombic Lip in Mouse Cerebellar Development." *J Neurosci* 34.37 (2014): 12527-37. Print.

Zecevic, N., and P. Rakic. "Differentiation of Purkinje Cells and Their Relationship to Other Components of Developing Cerebellar Cortex in Man." *J Comp Neurol* 167.1 (1976): 27-47. Print.

Zhao, X., et al. "The N-Myc-Dll3 Cascade Is Suppressed by the Ubiquitin Ligase Huwe1 to Inhibit Proliferation and Promote Neurogenesis in the Developing Brain." *Dev Cell* 17.2 (2009): 210-21. Print.

Zhao, X., et al. "The Hect-Domain Ubiquitin Ligase Huwe1 Controls Neural Differentiation and Proliferation by Destabilizing the N-Myc Oncoprotein." *Nat Cell Biol* 10.6 (2008): 643-53. Print.